Palacký University Olomouc

Faculty of Science

Department of Cell Biology and Genetics

Autophagy induction decreases the presence of endogenous P301S tau aggregates

Bachelor Thesis

Jiří Hrubý

Study program: Biology

Field of Study: Molecular and Cell Biology

Form of Study: Full-time

Olomouc 2020

Supervisor: Mgr. Narendran Annadurai

Bibliographical identification:

Author's first name and surname	Jiří Hrubý
Title	Autophagy induction decreases the presence of endogenous P301S tau aggregates
Type of thesis	Bachelor
Department	Department of Cell Biology and Genetics
Supervisor	Mgr. Narendran Annadurai
The year of presentation	2020
Keywords	Alzheimer's disease, autophagy, tauopathy, tau, protein aggregates
Number of pages	viii, 34 pp.
Language	English

Summary:

Aging-associated neurodegenerative diseases are becoming more prevalent in the modern society, and many of which belong to the group of tauopathies, characterized by the presence of aggregates of misfolded microtubule-associated protein tau. In brains of patients afflicted with Alzheimer's disease, there is a decrease, and failure in cellular autophagy mechanisms. Such decrease or failure in the protein aggregate clearance systems leads to progressive accumulation of toxic protein species. It was suggested that the induction of autophagy could be used as a possible treatment of tauopathies. The aim of the thesis was to test whether autophagy in Tau P301S biosensor cells is decreased by the presence of extracellular R3 tau aggregates induced-intracellular P301S tau aggregates and if induction of autophagy in these cells would lead to the clearance of these intracellular P301S tau aggregates. Epigallocatechin gallate (EGCG), a catechin found in green tea leaves, was used as an autophagy inducer. Transfection of Tau P301S biosensor cells with R3 tau aggregates was conducted by liposome-mediated transfection and the reduction of autophagy was examined by western blotting with autophagy markers such as LC3AB, p62/SQSTM1, and LAMP1. The IC_{50} value of EGCG was determined by an MTT assay. The decrease in the aggregation of endogenous phosphorylated pSer262 tau was tested by western blotting and fluorescent microscopy. Results show that in the presence of extracellular R3 aggregates inside the cells, autophagy deteriorated over time, resulted in an increase of endogenous Tau-RD aggregates and EGCG treatment resulted in an increase of autophagy and a decrease in the levels of triton-insoluble Ser262 phosphorylated intracellular P301S tau aggregates.

Bibliografická identifikace:

Jméno a příjmení autora	Jiří Hrubý
Název práce	Indukce autofagie snižuje přítomnost endogenních P301S tau agregátů
Typ práce	Bakalářská
Pracoviště	Katedra buněčné biologie a genetiky
Vedoucí práce	Mgr. Narendran Annadurai
Rok obhajoby práce	2020
Klíčová slova	Alzheimerova choroba, autofagie, tauopatie, tau, proteinové agregáty
Počet stran	viii, 34 s.
Jazyk	Angličtina

Souhrn:

Neurodegenerativní choroby spojené se stárnutím se v moderní společnosti stávají častějšími, a mnoho z nich patří do skupiny tauopatií, charakterizovaných přítomností agregátů špatně složeného s mikrotubuly asociovaného proteinu tau. V mozcích pacientů postižených Alzheimerovou chorobou, dochází k snížení a selhávání mechanismů buněčné autofagie. Tento úbytek nebo selhání v odstraňování agregátů proteinů vede k postupné akumulaci toxických druhů proteinů. Ukazuje se, že podpoření autofagie by mohlo být možným léčebným postupem při léčbě tauopatií. Cílem této práce bylo otestovat, jestli u buněčné linie Tau P301S biosensor je autofagie v přítomnosti intracelulárních P301S tau agregátů, indukovaných extracelulárními R3 tau agregáty, snížená a jestli by indukce autofagie vedla k odstranění těchto P301S tau agregátů. Jako induktor autofagie byl použit epigallokatechin gallát (EGCG), katechin přítomný v listech zeleného čaje. Buňky byly transfekovány R3 tau agregáty pomocí liposomové transfekce a pokles autofagie byl vyhodnocen pomocí western blotu detekcí markerů autofagie – LC3A/B, p62/SQSTM1 a LAMP1. Hodnota IC_{50} EGCG byla stanovena využitím MTT testu. Pokles endogenních pSer262 tau agregátů byl testován pomocí western blotu a fluorescenční mikroskopie. Výsledky ukázaly, že v přítomnosti extracelulárních R3 tau agregátů buněk dochází k postupnému poklesu autofagie, vedoucí k nárůstu endogenních tau-RD agregátů a po působení EGCG bylo dosaženo nárůstu autofagie a snížení hladiny v tritonu nerozpustných intracelulárních P301S tau agregátů fosforylovaných na Ser262.

"I declare that this Bachelor Thesis was developed independently, under the guidance of my supervisor, and by using the cited literature."

In Olomouc, ……..…….. Signature ……..……..

ACKNOWLEDGMENT

This Bachelor thesis was performed at the Institute of Molecular and Translational Medicine in Olomouc, in collaboration with the Palacký University in Olomouc.

I would like to thank my supervisor, Mgr. Narendran Annadurai, for his everlasting patience and friendly attitude, for teaching me new skills and showing me a whole new field of interest.

I would also like to thank Mgr. Anna Janošťáková of Laboratory of Tissue Culture for her thoughtful advice during my experiments and introducing me to the world of cell culturing. And finally, I would like to thank my family and friends for their support and patience during my studies.

TABLE OF CONTENTS

ACKNOWLEDGMENT iv

LIST OF ABBREVIATIONS vii

LIST OF FIGURES viii

1 INTRODUCTION 1

2 AIM OF THESIS 2

3 LITERARY REVIEW 3

3.1 Microtubule-associated protein tau 3

3.1.1 Structure of tau protein 3

3.1.2 Tau properties and function 4

3.1.3 Posttranslational modifications of tau protein 5

3.2 Tau pathology, tauopathies 6

3.2.1 Tau protein degradation 6

3.2.2 Tau aggregates and their propagation 7

3.2.3 Tau toxicity 8

3.2.4 Tauopathies 9

3.3 Autophagy 11

3.3.1 What is autophagy? 11

3.3.2 Autophagy mechanism 13

3.3.3 Autophagy regulation 14

3.3.4 Autophagy in Alzheimer's disease 15

3.3.5 Tau aggregation and Autophagy 16

4 MATERIALS AND METHODS 18

4.1 Cell-line 18

4.2 Equipments 18

4.3 Chemicals and solutions 18

4.4 Antibodies 19

4.5 Methods 20

5 RESULTS 23

5.1 Determining the IC_{50} value of EGCG 23

5.2 Seeding Tau P301S biosensor cells with Tau R3 aggregates 23

5.3 Analysis of autophagy levels after seeding with Tau R3 aggregates 23

5.4 EGCG induced autophagy reduced the level of Tau R3 aggregate induced triton-insoluble intracellular pSer262 Tau P301S aggregate 23

6 DISCUSSION 29

7 CONCLUSION 30

REFERENCES 31

LIST OF ABBREVIATIONS

0N/1N/2N	Number of N-terminal domain inserts of tau protein
3R/4R	Number of microtubule-binding domain repeats of tau protein
AD	Alzheimer's disease
APP	Amyloid precursor protein
ATG	Autophagy-related
CBD	Corticobasal dementia
CMA	Chaperone-mediated autophagy
HDAC6	Histone deacetylase 6
LAMP	Lysosome associated membrane protein
LC3	Microtubule-associated protein 1 light chain 3
MAPT	Microtubule-associated protein tau
mTORC1	Mammalian target of rapamycin
N1/N2	Distinct N-terminal domain inserts of tau protein
NFTs	Neurofibrillary tangles
PD	Parkinson's disease
PHFs	Paired helical filaments
PKA	cAMP-dependent protein kinase A
PSN1	Presenilin 1
PSP	Progressive supranuclear palsy
R1/R2/R3/R4	Distinct microtubule-binding domain repeats of tau protein
SQSTM1/p62	Sequestosome 1/protein 62
TOR	Target of rapamycin
ULK	Unc-51-like kinase
SNAREs	SNAP receptors

LIST OF FIGURES

Figure 1: The schematic structure of tau isoforms 3

Figure 2: A- Schematic drawing of tau; B - Paperclip conformation of free tau; C - Phosphorylated free tau; D - Tau bound to microtubule 5

Figure 3: Distinct types of autophagy 12

Figure 4: Mechanism of phagophore formation and creation of autophagosome 14

Figure 5: Degradation of hyperphosphorylated tau based on the number of N-terminal repeats..... 17

Figure 6: Effect of EGCG on cell viability 24

Figure 7: Western blot analysis of LC3A/B, p62, and LAMP1 levels after seeding R3 aggregates into Tau P301S biosensor cells..... 25

Figure 8: Western blot analysis of LC3A/B, p62, and LAMP1 levels after 48 hours EGCG treatment of R3 aggregates seeded Tau P301S biosensor cells 26

Figure 9: A- Intracellular R3 aggregates seeded tau aggregate inclusions under different concentrations of EGCG treament. B- Analysis of number of tau aggregregates in R3 aggregates seeded tau P301S biosensor cells after EGCG treatment 27

Figure 10: Western blot and levels of triton-soluble and triton-insoluble pSer262 tau of R3 aggregates seeded Tau P301S biosensor cells..... 28

1 INTRODUCTION

According to Alzheimer's disease International (2019) ("World Alzheimer Report 2019: Attitudes to dementia.," Alzheimer's Disease International, London, UK.), it is estimated that over 50 million people live with dementia all over the world and this number is expected to rise to ca. 152 million by 2050 as the world population ages. Dementia and other neurodegenerative diseases are often characterized by the accumulation of misfolded proteins. A heterogeneous group of neurodegenerative diseases, collectively called tauopathies, is characterized by the presence of aberrant, misfolded hyperphosphorylated microtubule-associated protein tau (Guo *et al*., 2017). This protein is crucial for neuronal cytoskeletal dynamics and overall neuronal function. Furthermore, when aberrantly expressed, tau can induce cytotoxicity and even spread from cell to cell, like prion protein (Gibbons *et al.*, 2019). In Alzheimer's disease (AD), tau progressively accumulates in the brain partly due to a damaged protein clearance mechanisms such as autophagy (Caberlotto *et al.*, 2019). These clearance mechanisms deteriorate with age (Eskelinen, 2019), explaining the progressive increase of numbers of dementia cases in our modern long-lived society. Several studies have shown that the induction of autophagy is beneficial in the clearance of misfolded protein aggregates. Hence, finding a proper autophagy inducer is a promising way for dementia treatment (Pierzynowska *et al.*, 2018). That is why we have decided to test autophagy induction and tau aggregate clearance in this thesis. We hope thatthe results will shed some light on this problem and give suggestion a possible way to approach further studies in the future.

2 AIM OF THESIS

In this thesis, I studied whether autophagy is affected in the Tau P301S biosensor cells that are seeded with extracellular R3 tau aggregates, and if induction of autophagy leads to the clearance of intracellular P301S tau aggregates . The study was conducted by utilizing *in vitro* methods of cell culturing, cell toxicity MTT assay, transfection, fluorescence microscopy, and western blotting.

3 LITERATURE REVIEW

3.1 Microtubule-associated protein tau

3.1.1 Structure of tau protein

Tau is a microtubule-associated protein, found abundantly in axons (Barbier *et al.*, 2019), plasma membrane, nucleus, mitochondria, and other parts of neurons (Guo *et al.*, 2017). It is also expressed in small quantities in glial cells (Gibbons *et al.*, 2019). Tau is encoded by *MAPT* (microtubule-associated protein tau) gene located on chromosome 17, which is composed of 16 exons. In humans, six different tau isoforms are expressed due to alternative splicing of *MAPT* gene at exon 2, 3, and 10 (Guo *et al.*, 2017). Two distinguished haplotypes, called H1 and H2, are characterized based on whether the gene is in inverted orientation or not (Zhang *et al.*, 2018).

Depending on the type of neuron and the stage of its maturation, *MAPT* pre-mRNA is spliced differently (Guo *et al.*, 2017). Tau isoforms are different in their inner structure, and differ by the number of N-terminal inserts and microtubule-binding repeats present in the protein (Fig. 1). Tau isoforms have 0, 1 or 2 N-terminal inserts (0N, 1N or 2N), and three or four microtubule-binding repeats (3R or 4R) near the C-terminus (Barbier *et al.*, 2019). These regions are flanked by a proline-rich domain (Gibbons *et al.*, 2019; Guo *et al.*, 2017). All isoforms are expressed in adults, whereas only the shortest (0N3R) isoform is expressed in the fetal brain (Guo *et al.*, 2017). The expression of tau isoforms differs in different cerebral regions. (Guo *et al.*, 2017), and a healthy adult human brain expresses both 3R and 4R isoforms at equal ratio (Hanger *et al.*, 2009).

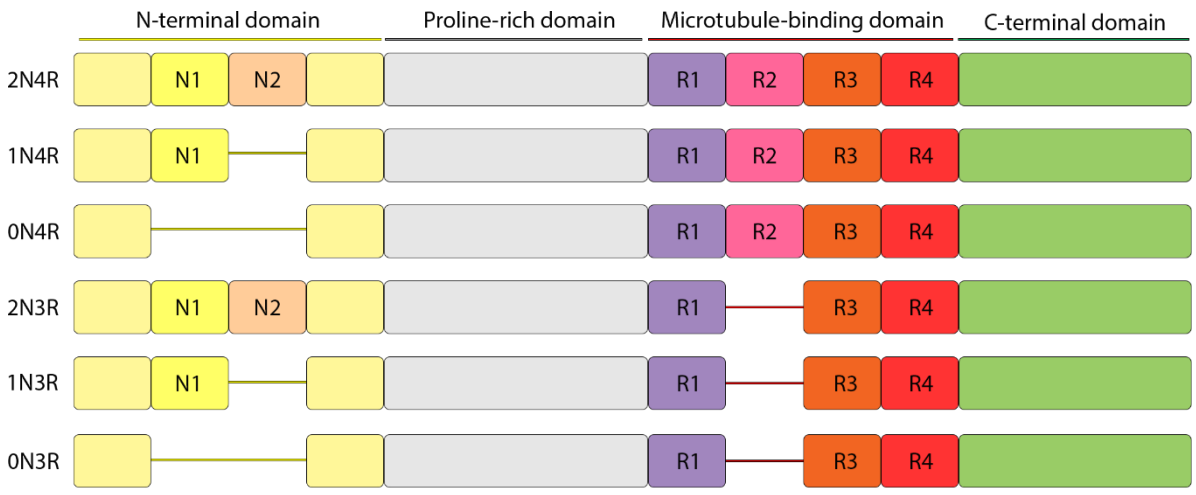

Figure 1: The schematic structure of tau isoforms. Distinct domains are highlighted by different colors.

3.1.2 Tau properties and function

The primary role of tau protein is to stabilize microtubules increasing their growth rate, and preventing their dissociation in neurons (Barbier *et al.*, 2019). It has also demonstrated the ability to induce microtubule and tubulin rings assembly, without tubulin self-assembly. Hence, apart from being a microtubule stabilizer, tau protein may serve as a microtubule-assembly inducer (Barbier *et al.*, 2019).

Apart from the cytosolic microtubule-associated fraction, a nuclear fraction was also found. In the nucleus, tau may have several functions. In primary neurons, tau exhibits a characteristic similar to heat shock protein 70 when cytoplasmic tau translocates to the nucleus upon heat stress, protecting DNA integrity. It binds to DNA at AT-rich minor grooves via proline-rich domain and microtubule-binding repeats (Guo *et al.*, 2017). Findings (reviewed by (Guo *et al.*, 2017)) proposes that tau might be involved in epigenetic regulation of gene expression.

Tau is an intrinsically disordered protein with highly flexible conformation, with a very low to zero significant secondary structure, except for local β-strands in microtubule-binding repeats and polyproline helices in the proline-rich region (Barbier *et al.*, 2019). It is proposed that when not bound to the microtubule, tau tends to be in "paperclip" conformation (Fig. 2B), with the C-terminus folding over the microtubule-binding domain and the N-terminus folding over the C-terminus (Barbier *et al.*, 2019; Guo *et al.*, 2017). When bound to the microtubule, N-terminus projects away from microtubule (Fig. 2D). Even when not directly interacting with microtubules, tau is important for microtubule dynamics. For example, it is involved in axonal transport-inhibiting cascade (Guo *et al.*, 2017), and it has been proposed that it interacts with the neuronal plasma membrane (Andreadis, 2006), probably through interaction with the membrane-binding protein annexin A2 (Guo *et al.*, 2017). It has been also shown to interact with dynein and other motor proteins (Guo *et al.*, 2017). The proline-rich domain of tau involved in protein-protein interaction, modulation of signal transduction, regulation of microtubule assembly, and binding to actin, plays an important role in neuronal cytoskeleton dynamics. It also serves as a DNA and RNA interacting site (Guo *et al.*, 2017). Tau protein interacts with microtubules through microtubule-binding repeats (Gibbons *et al.*, 2019; Guo *et al.*, 2017), although a single microtubule-binding repeat does not bind and assemble microtubules as effectively as the whole tau protein (Barbier *et al.*, 2019). 3R isoforms have a lower affinity for microtubules than their 4R counterparts (Hanger *et al.*, 2009). Tau exhibits the ability to bind to F-actin and to crosslink microtubule and actin cytoskeletons, thus being crucial for the proper function of the neuronal cytoskeletal system (Elie *et al.*, 2015). It also interacts with α-synuclein, presenilin 1, apolipoprotein E, histone deacetylase 6 (HDAC6), DNA and RNA (Guo *et al.*, 2017). Apart from the N-terminal region, tau can interact with neuronal lipid bilayers, including the plasma membrane through microtubule-binding repeats (Georgieva *et al.*, 2014; Guo *et al.*, 2017).

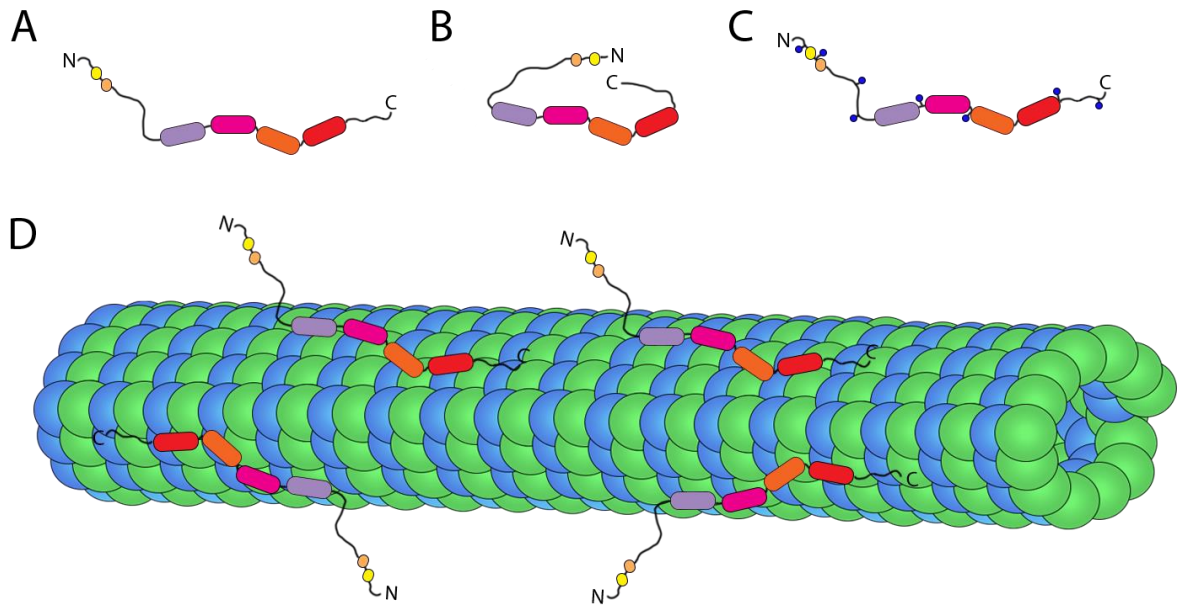

Figure 2: A- schematic drawing of tau; B - paperclip conformation of free tau; C - phosphorylated free tau; D - tau bound to microtubule by its microtubule-binding domain with the N-terminal domain projecting away from microtubule.

3.1.3 Posttranslational modifications of tau protein

The ability of tau to bind to and stabilize microtubules and its other functions are dependent on the level of posttranslational modifications like phosphorylation, acetylation, N-glycosylation, glycation and others (Guo *et al.*, 2017). Phosphorylation of tau is the prevalently described tau modification (Guo *et al.*, 2017). It negatively regulates the affinity of tau to microtubules. In normal conditions, the level of tau phosphorylation is low and a proper microtubule function is maintained. Pathological disbalance between protein kinases and phosphatases leads to hyperphosphorylation, thereby debilitating its microtubule-stabilizing function (Fan *et al.*, 2020). Tau has 85 phosphorylation sites, consisting of 45 serine, 35 threonine, and 5 tyrosine residues (Hanger *et al.*, 2009). The level of phosphorylation in the microtubule-binding repeats is thought to be imperative in its microtubule-binding ability. For example, phosphorylation at Ser262, Ser293, Ser324, and Ser356 residues detaches tau from microtubules (Guo *et al.*, 2017; Hanger *et al.*, 2009).

Tau is phosphorylated by kinases, which can be divided into three groups: 1) proline-directed serine/threonine kinases such as glycogen synthase kinase (GSK), cyclin-dependent kinase 5 (Cdk5), mitogen-activated protein kinases (MAPKs) and others, 2) non-proline-directed kinases, such as tau-tubulin kinase 1/2, casein kinase 1, microtubule affinity regulating kinases (MARKs), protein kinase C and others, and 3) tyrosine residues specific kinases, such as Src or Fyn (Guo *et al.*, 2017). Dephosphorylation of tau is performed by protein phosphatase 2A (PP2A) and protein phosphatase 5 (Guo *et al.*, 2017). The level of phosphorylation is different in the fetal

and adult brain. In adults, tau manifests a lower level of phosphorylation as opposed to the fetal brain. It might be due to higher demand for neuronal plasticity during embryonal and fetal CNS development and the need for dynamic cytoskeleton for synaptogenesis (Hanger *et al.*, 2009).

Acetylation is another posttranslational modification of tau (Guo *et al.*, 2017), and is performed by cAMP-response binding protein-binding protein (CBP) and acetyltransferase p300, whereas deacetylation by sirtuin 1 (SIRT1) and HDAC6. Tau also displays intrinsic autoacetyltransferase activity mediated by Cys291 residue, located in R2 microtubule-binding repeat, and Cys322 residue, located in R3 repeat (Cohen *et al.*, 2013). This activity is exhibited only in the free unbound form of tau because through these residues, tau binds to tubulin of microtubules. Autoacetylation targets lysine residues located in the microtubule-binding repeats, whereas CBP acetylates lysine residues in both microtubule-binding repeats and proline-rich regions (Cohen *et al.*, 2016).

3.2 Tau pathology, tauopathies

Under physiological conditions, tau protein in neuronal axons is highly soluble (Hanger *et al.*, 2009) and its function depends on posttranslational modifications, mostly phosphorylation. Hyperphosphorylation can impair axonal transport and induce neurotoxicity (Barbier *et al.*, 2019; Fan *et al.*, 2020).

Hyperphosphorylated tau accumulates in the cells and forms insoluble paired helical filaments (PHFs) and straight filaments, which then lead to the formation of intraneuronal neurofibrillary tangles (NFTs), fibrillar deposits of defective tau that reduce the number of synapses (Fan *et al.*, 2020). However, studies have shown that small soluble phosphorylated tau is more toxic in tau pathology (commonly called tauopathy) since it can spread between cells more easily than NFTs. Not only hyperphosphorylated tau but acetylated tau and truncated tau can have also pathological significance (Fan *et al.*, 2020). *MAPT* mutations can also cause tau protein abnormalities leading to neurodegeneration (Guo *et al.*, 2017).

3.2.1 Tau protein degradation

Tau is degraded by enzymes, the ubiquitin-proteasome system, and autophagy (Guo *et al.*, 2017; Rubinsztein, 2006). Caspases, calpains, thrombin, puromycin-sensitive aminopeptidase, and many other proteases aim for tau. However, enzymatic truncation of tau may add to the pathology either since truncated tau may be toxic or proteases regulation may be defunct. The ubiquitin-proteasome system seems to be inhibited in tauopathies, further aggravating tau accumulation (Guo *et al.*, 2017). Surprisingly, soluble tau in normal conditions is degraded by the ubiquitin-proteasome system. Autophagy is crucial for the clearance of pathological species of tau (Rodríguez-Martín *et al.*, 2013; Rubinsztein, 2006), and it also degrades truncated fragments (Rodríguez-Martín *et al.*, 2013). Tau clearance is dependent on its posttranslational modifications. For example, tau phosphorylated on

Ser262 or Ser356 residues is not degraded by the proteasomal pathway, since it is not recognized by heat shock protein complex important for proteasomal degradation (Guo *et al.*, 2017). Interestingly, phosphomimetic tau (tau modified on its phosphorylation sites by glutamate or aspartate) is degraded by autophagy (Rodríguez-Martín *et al.*, 2013).

3.2.2 Tau aggregates and their propagation

The tendency of tau to aggregate is influenced by two hexapeptide motifs in its microtubule-binding region (Seidler *et al.*, 2018). These VQIXXK motifs are in second and third microtubule-binding repeat: PHF6 in R3 repeat residues ^{306}-VQIVYK-^{311} and PHF6* in R2 repeat residues ^{277}-VQIINK-^{280} (Li and Lee, 2006). These motifs have the tendencies to self–assemble into β-sheet structures (Guo *et al.*, 2017), and both motifs contribute to tau fibrils formation (Li and Lee, 2006). PHF6 in 3R is required for tau fibrillization, whereas PHF6* enhances the process (Li and Lee, 2006; Seidler *et al.*, 2018). Because of this, 4R tau isoforms with R2 repeat with PHF6* are more prone to aggregation than 3R isoforms. Tau dimerization is possible between two PHF6 motifs, two PHF6* motifs, or PHF6 and PHF6* (Guo *et al.*, 2017). Recruitment of tau molecules to PHFs leads to the creation of a nucleation center, thus enabling tau oligomerization and formation of β-sheet-rich fibrils ,which progressively form NFTs (Guo *et al.*, 2017). Disruption of VQIXXK motifs by mutations can hinder its self-assembly ability and thus decrease aggregation. By contrast, other mutations such as P301L or ΔK280 intensify the aggregation propensity (Wang and Mandelkow, 2016).

Aggregation propensity of tau is altered by a change in its overall positive charge (Guo *et al.*, 2017), and this results either due to mutations or posttranslational modifications (Wang and Mandelkow, 2016). Mutations of *MAPT* can be classified as missense mutations that result in various tau mutants and splicing mutations that affect the ratio of isoform (Wang and Mandelkow, 2016). Missense mutations tend to decrease tau microtubule-binding ability, increasing the aggregation. Most pathological mutations such as P301L or ΔK280 are located in or near the microtubule-binding domain, while others such as A152T localizes in the proline rich region (Wang and Mandelkow, 2016). Interestingly, A152T mutant tau tends to create oligomers but no fibers (Wang and Mandelkow, 2016). Splicing mutations are near intron 10, leading either to the inclusion or exclusion of R2 in the encoded protein, resulting in impaired 4R/3R ratio (Hanger *et al.*, 2007; Wang and Mandelkow, 2016). Hyperphosphorylation of tau gradually increases the negative charge of tau, and acetylation leads to neutralization of positively-charged lysine residues (Guo *et al.*, 2017; Wang and Mandelkow, 2016). Truncated tau fragments can also create tau oligomers and fibrils (Guo *et al.*, 2017), especially segments containing the microtubule-binding repeat domain (Wang and Mandelkow, 2016).

Tau displays prion-like properties (Guo *et al.*, 2017), which has been proved in several experimental studies (Gibbons *et al.*, 2019; Guo *et al.*, 2017). Although tau displays prion-like properties, unlike real prions, there is no evidence to suggest that tau transmission is infectious, (Gibbons *et al.*, 2019).

P301L tau transgenic mice expressing tau primarily in the entorhinal cortex suffer from the spread of misfolded tau to CA1 region of the hippocampus and into dentate gyrus (Guo *et al.*, 2017). Mouse brains injected with P301S tau isolated from brains of transgenic mice or human tauopathy patients develop tau aggregates not only in the place of injection but even further from the sitein neurons that connected to the neurons close to the place of injection (Guo *et al.*, 2017). This suggest a transsynaptic transmission of tau pathology. Furthermore, injection of tau derived from different human tauopathies has shown that specific strains of tau have cell-type selectivity, afflicting regions specific for the given tauopathy (Gibbons *et al.*, 2019; Guo *et al.*, 2017). Tau can also be secreted, transmitted, and taken up by neurons in ways other than transsynaptic (Gibbons *et al.*, 2019; Guo *et al.*, 2017) . Tau can be released from cells in vesicles or as free soluble tau. This correlates with clinical observations where hyperphosphorylated tau is detected in cerebrospinal fluid of AD patients andhealthy individuals (Gibbons *et al.*, 2019). Tau is also released in the medium by tau-expressing cells even in the absence of cell death (Guo *et al.*, 2017). Tau is taken up by pinocytosis, endocytosis, or membrane fusion (Gibbons *et al.*, 2019). Tunneling nanotubes are also suggested as a possible pathway for tau spreading (Guo *et al.*, 2017). Truncation, fragmentation, and oligomerization has also shown to increase its ability to propagate and aggregate (Guo *et al.*, 2017).

3.2.3 Tau toxicity

Dysfunctional tau can be toxic either due to the loss of function or toxic gain of function. Mutated and hyperphosphorylated, acetylated, aggregated, and/or truncated tau cannot bind properly to microtubules and this may cause microtubule disassembly (Wang and Mandelkow, 2016). Tau aggregation also decreases the intracellular level of soluble tau, further debilitating microtubules (Guo *et al.*, 2017; Wang and Mandelkow, 2016). Disassembly of the microtubule network impairs anterograde and retrograde axonal transport in neurons. Since tau competes with kinesin and dynein for binding to microtubules, tau overexpression can alter axonal transport leading tothe accumulation of cellular cargo in cell soma and synaptic degeneration(Guo *et al.*, 2017; Wang and Mandelkow, 2016). Furthermore, tau is mislocalized into dendritic compartments (Guo *et al.*, 2017; Wang and Mandelkow, 2016). Dendritic tau can affect axonal transport by its interaction with enzymes, katanin and spastin (Guo *et al.*, 2017). When bound to axonal microtubules, tau protects microtubules from the influence of katanin and thus impede depolymerization. Dendritic tau, however, engages tubulin tyrosine ligase–like 6 (TTLL6), which then mislocalizes to dendrites. In dendrites, TTLL6 polyglutamylates the microtubules, which are then prone to cleavage by spastin (Guo *et al.*, 2017; Wang and Mandelkow, 2016).

High levels of tau can also impact mitochondrial localization and function (Guo *et al.*, 2017). Mitochondria count in axons was decreased in mutant P301L knock-in mice and the level of reactive oxygen species was increased (Guo *et al.*, 2017). Also, tau truncated at Asp421 has shown to disrupt mitochondrial integrity. Mitophagy (autophagy of mitochondria) indicators, like cytochrome c

oxidase IV or mitochondrial DNA, have been detected in both AD patients' brains and transgenic mouse models. Besides, overexpression of tau leads to defective mitophagy and disruption of proper mitochondrial function (Guo *et al.*, 2017). Nuclear tau, when defective, can lose its DNA protecting function, aggravating cellular stress and making cells prone to chromosome aberrations, improper gene expression and even to cell-cycle re-entry (Guo *et al.*, 2017).

Evidence shows that NFTs are not necessary for neurodegeneration (Wang and Mandelkow, 2016). In AD patients, NFTs distribution correlates with the level of cognitive impairment but does not correlate with the neuronal death. This was also proven in transgenic mice (Wang and Mandelkow, 2016). NFTs themselves also do not cause synaptic decay, since defective cognition and synaptic damage occur even before appearance of NFTs (Wang and Mandelkow, 2016). There are also suggestions that highly aggregated NFTs may be protective for neurons, since aggregates may serve as scavengers for tau fragments, oligomers, and monomers and thus, for example, protect mitochondria from damage (Guo *et al.*, 2017; Wang and Mandelkow, 2016). This suggests that PHFs, oligomers, and other more soluble forms are more toxic than NFTs. However, NFTs still are neurotoxic since they may cause aggregation of normal tau, affect the balance between 3R and 4R isomers and, when not being cleared from cells, occupy intracellular space and inhibit cellular function (Guo *et al.*, 2017; Wang and Mandelkow, 2016). The main trait of tau to cause its toxicity seems to be its ability to aggregate. This claim has been proven in a comparative study of transgenic mouse models (Wang and Mandelkow, 2016) producing human full-length tau or its microtubule-binding repeat domain either with pro-aggregatant ΔK280 mutation or with proline substitutions disrupting its β-sheet structure tendency. Pro-aggregatant mutants developed neurodegenerative AD-like pathology, while the non-aggregant mutants developed almost no pathology.

3.2.4 Tauopathies

Tauopathies are a heterogeneous group of complex dementia and movement disorders, in which a high concentration of hyperphosphorylated forms of tau can be found in the patient's neural system (Guo *et al.*, 2017). Alzheimer's disease, Parkinson's disease (PD), Pick's disease, frontotemporal lobar dementia, Lewy body dementia, Huntington's disease, and many others belong to this category (Guo *et al.*, 2017; Jucker and Walker, 2013). It is not uncommon for tauopathies to be accompanied by other abnormal proteins. For example, AD patiens also how the aberrant deposition of amyloid-β aggregate. In PD, there is aggregated α-synuclein and in Huntington's disease, huntingtin is mutated. Moreover, pathologies of the distinct disease can intertwine. Lewy body-spherical aggregates of α-synuclein are accompanied by other proteins aggregates including tau (Ishizawa *et al.*, 2003) have been detected in more than half brain autopsies of AD patients. Half of PD brains exhibit tau and amyloid-β pathology, large big enough to be diagnosed as AD (Guo *et al.*, 2017).

AD is characterized by the presence of deposits of amyloid-β that form the extracellular senile plaques, and intracellular NFTs of tau (Scheltens *et al.*, 2016). Two hypotheses propose possible pathways leading to AD which consider defective amyloid-β and tau protein - amyloid cascade hypothesis and tau hyperphosphorylation hypothesis (Fan *et al.*, 2020). The amyloid cascade hypothesis proposes that the formation and deposition of amyloid-β initiate events leading to dementia and is a crucial point leading to AD (Karran *et al.*, 2011). This hypothesis has become a dominant model for AD research and treatment development (Selkoe and Hardy, 2016). Amyloid-β, apart from being prion-like protein (Jucker and Walker, 2013), can also activate a cascade of protein kinases, such as liver serine/threonine kinase and microtubule affinity-regulating kinases (MARKs), which can lead to abnormal tau phosphorylation (Annadurai *et al.*, 2017; Fan *et al.*, 2020). Unlike amyloid-β plaque formation, the level of tau pathology is responsible for cognitive impairment and correlates with this affliction (Fan *et al.*, 2020). In AD, tau mislocalization into dendrites happens and this may mediate amyloid-β induced toxicity. Dendritic tau may serve as a scaffold for Fyn kinase delivery to postsynaptic sites, where this enzyme phosphorylates NMDA-receptor, thus making neurons susceptible to glutamatergic excitotoxicity (Guo *et al.*, 2017; Wang and Mandelkow, 2016). NTFs in AD are comprised mainly of hyperphosphorylated tau as well as several forms of truncated tau (Guo *et al.*, 2017) and in AD patients, the NFTs consists of all six isoforms of tau (Gibbons *et al.*, 2019).

Many tauopathies are accompanied by misfolded α-synuclein, namely PD, Parkinson's disease dementia, and a group of syndromes called Parkinson-plus syndromes. *MAPT* locus is one of the most significant loci affecting PD (Guo *et al.*, 2017). Even though PD was not considered a tauopathy (Zhang *et al.*, 2018), tau could act as the driver of neurodegeneration in parkinsonism independent of α-synuclein (Guo *et al.*, 2017). NFTs are colocalized with Lewy bodies, bundles of aggregated α-synuclein, and tau fibrils are even incorporated in Lewy bodies (Guo *et al.*, 2017). *In vitro* tau displays faster fibrillization when incubated with α-synuclein, and α-synuclein toxicity, secretion, and inclusion creation was enhanced in human neuroglioma and primary neuronal cultures (Guo *et al.*, 2017). Coincubation of α-synuclein and tau also has been shown to promote the assembly of tau into NFTs and even phosphorylation of tau (Zhang *et al.*, 2018). The mechanisms for this intriguing relationship between tau and α-synuclein remains to be elucidated (Zhang *et al.*, 2018).

Some diseases related to PD, such as frontotemporal dementia-17 with Parkinsonism (familial frontotemporal dementia) is directly caused by dominantly inherited *MAPT* mutations (Zhang *et al.*, 2018), or corticobasal dementia (CBD) or progressive supranuclear palsy (PSP). The latter two are PD subtypes, called Parkinson-plus syndromes (Zhang *et al.*, 2018). They have distinct features in morphology and biochemical properties, but both are characterized by the presence of 4R tau tangles in neurons and glial cells (Gibbons *et al.*, 2019). In Pick disease, both glia and neurons are affected by Pick bodies, which are dense spherical bundles of tau protein. Unlike PSP or CBD, Pick disease is characterized by the presence of aggregates of 3R isoforms

(Gibbons *et al.*, 2019). CBD, PSP and Pick disease are also referred to as frontotemporal lobar degeneration-tau (Dickson *et al.*, 2011). They are complex syndromes, and their symptoms and pathologies can overlap, hence they are difficult to diagnose (Dickson *et al.*, 2011; Golbe, 2014).

In primary age-related tauopathy, NFTs consisting of both 3R and 4R isoforms are present in patients, similarly to AD, but without or with very low amyloid-β depositions. However, it is not clear yet whether this is a distinct tauopathy or an early stage of AD (Gibbons *et al.*, 2019).

3.3 Autophagy

3.3.1 What is autophagy?

Autophagy is a cellular defense mechanism for the clearance of misfolded and damaged cell organelles along with the ubiquitin-proteasome system (Rubinsztein, 2006). In autophagy, enzymes in lysosomes are utilized, for example *via* its fusion with *de novo* created membranous compartment - autophagosome (Glick *et al.*, 2010). We distinguish three types of autophagy: macroautophagy, microautophagy, and chaperone-mediated autophagy (Glick *et al.*, 2010). In macroautophagy, generally called autophagy (Rubinsztein, 2006), cargo targeted for degradation is engulfed by a double-membrane vesicle called the autophagosome, which is fused with a lysosome, forming the autophagolysosome. In microautophagy, molecules for degradation are uptaken by the lysosome itself, by the invagination of its membrane (Glick *et al.*, 2010). Both macro- and microautophagy can be either selective or non-selective, depending on whether specific molecule (e.g. misfolded protein) or organelle (e.g. worn-out mitochondria) in selective autophagy or bulk of cytoplasm and everything in it in non-selective autophagy is digested (Alberts, B., 2015). Non-selective autophagy is induced by serum starvation (Eskelinen, 2019). In chaperone-mediated autophagy, proteins for degradation are uptaken by lysosome when in complex with one of the chaperone proteins that are recognized by lysosome-associated membrane protein 2A (LAMP-2A), a lysosome membrane receptor (Glick *et al.*, 2010). Autophagosomes can alternatively fuse with recycling endosomes before fusing with a lysosome, forming an amphisome (Cheon *et al.*, 2019).

Autolysosomes have two possible clearance pathways. They can reform back to lysosomes or fuse with the plasma membrane and empty their contents into extracellular space (Eskelinen, 2019).

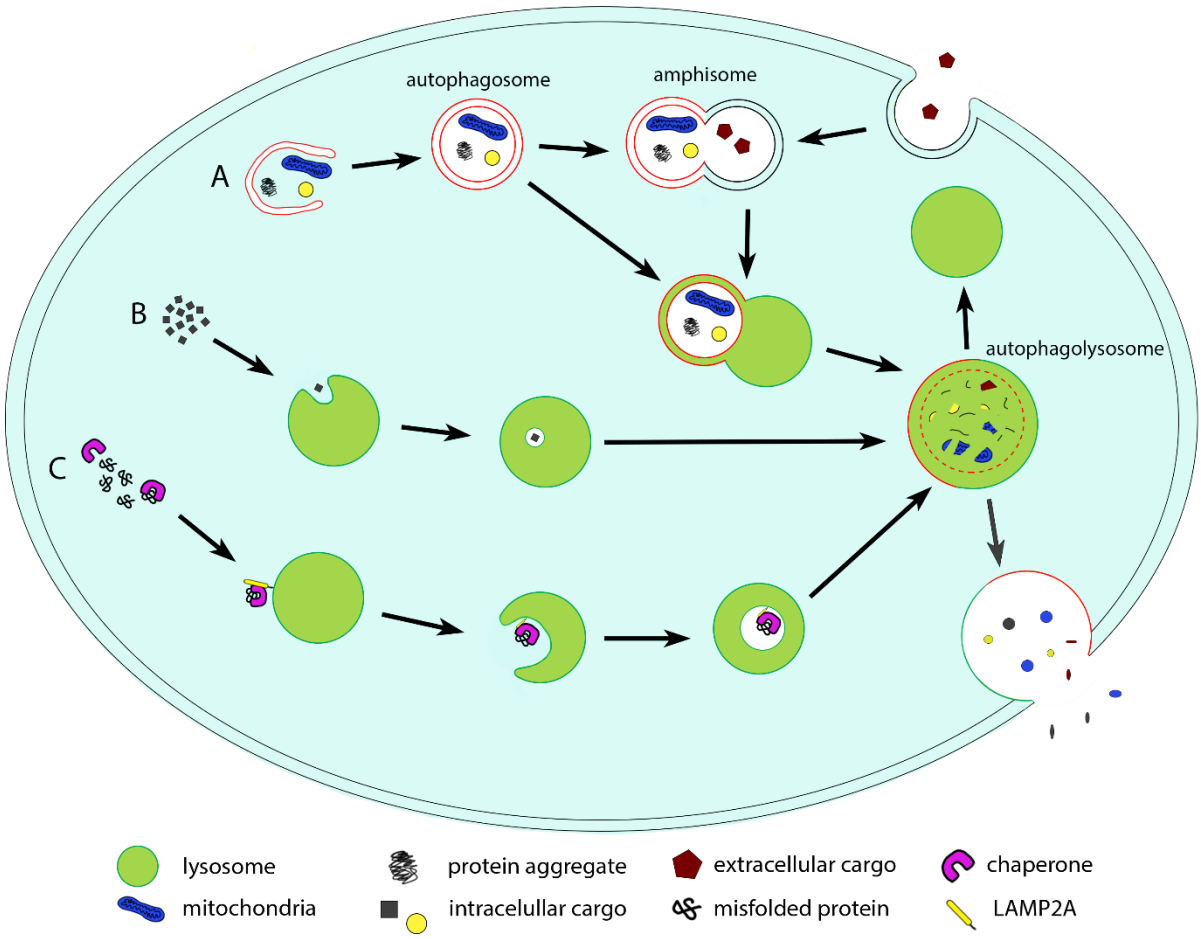

Figure 3: Distinct types of autophagy. A - macroautophagy: particular steps are: phagophore engulfing a part of the cytoplasm, forming of an autophagosome, alternatively fusion with endosome and forming an amphisome, fusion with the lysosome and forming the autophagolysosome, then either reforming of lysosome or release of degradation products to extracellular space; B - microautophagy, cargo is uptaken by lysosome itself and degraded; C - chaperone-mediated autophagy, a misfolded protein with a bound chaperone is uptaken by lysosome after recognition by LAMP2A receptor and degraded.

First autophagy genes (*ATG*) were discovered in mutant yeasts and analogous genes and proteins were found in mammals (Eskelinen, 2019). Analogous genes have also been identified in worms, flies, plants, and molds (Glick *et al.*, 2010).

Autophagy protects cells against stress and provides homeostasis. Post-mitotic cells, for example, neurons or muscle cells, are especially reliant on a high level of autophagy and clearance of damaged organelles and protein aggregates (Eskelinen, 2019). So, autophagic defects can lead to neurodegeneration, muscle diseases, even cancer or immunological and metabolic disorders (Cheon *et al.*, 2019; Eskelinen, 2019).

Neurodegenerative diseases characterized by the presence of misfolded proteins are connected to dysfunctional autophagy (Eskelinen, 2019). In PD, mutation of lysosomal type 5 ATPase ATP13A2 impairs lysosomal acidification and proteolysis, thus the autophagic clearance of α-synuclein aggregates. Furthermore, ATP13A2 promotes autophagosome-lysosome fusion, and stimulation of autophagy displayed α-synuclein pathology elevation (Eskelinen, 2019). In Huntington's disease, autophagic clearance of huntingtin is disabled (Eskelinen, 2019). Normally, huntingtin containing polyglutamine sequence is cleared *via* autophagy and has been recognized as an adaptor protein in selective autophagy by participating in the binding of p62/SQSTM1 to polyubiquitinylated cargo. However, huntingtin competitively disturbs interaction between Beclin1 and deubiquitinated ataxin, leading to faulty autophagosome formation (Eskelinen, 2019). Autophagy in AD is described further below.

3.3.2 Autophagy mechanism

First, signaling cascade informing about the metabolic status of the cell is inducted. In the early stage ULK (Unc-51-like kinase) complex, consisting of ULK1, ULK2, ATG13, FIP200, and ATG101 proteins, is activated and translocates into the endoplasmic reticulum (Cheon *et al.*, 2019; Eskelinen, 2019). The next step is activation of class III PI3K (phosphatidylinositol-3-kinase) complex, which contains Beclin1 and ATG14, apart from PI3-kinases and other proteins (Cheon *et al.*, 2019; Eskelinen, 2019). Thus phosphatidylinositol-3-phosphate (PI3P) is produced and an omegasome/phagophore, a special sub-compartment of endoplasmic reticulum, is created (Eskelinen, 2019). PI3P also affects WIPI (tryptophan-aspartic acid (WD) repeat domain phosphoinositide-interacting) proteins. WIPI recruits ATG12-ATG5-ATG16 complex to the phagophore (Cheon *et al.*, 2019; Eskelinen, 2019). The microtubule-associated protein 1 light chain 3 (LC3), a mammalian homolog of yeast ATG8 (Glick *et al.*, 2010) is cleaved by ATG4, becoming LC3I (Cheon *et al.*, 2019). LC3I is the lipidated in a ubiquitin-like manner to the phosphatidylethanolamine of the phagophore membrane by ATG7, ATG3, and ATG12-ATG5-ATG16 complex, becoming LC3II (Cheon *et al.*, 2019). Phagophore then via its elongation engulfs a compartment in the cytosol for degradation, forming the autophagosome, a double-layered membrane organelle (Glick *et al.*, 2010). ATG9-containing vesicles, recruited from either endosomes or Golgi, also contribute to autophagosome formation, but their exact function is not clear yet (Eskelinen, 2019). For the schematic drawing of phagophore formation, see Fig. 4. After its completion, autophagosome migrates along microtubules to the perinuclear area with the help of motor proteins kinesin and dynein (Cheon *et al.*, 2019), where lysosomes are located. Autophagosome-lysosome fusion is secured by several proteins, specifically HOPS (homeotypic fusion and vacuole protein sorting) complex, EPG5 (ectopic P granules protein 5), PLEKHM1 (pleckstrin homology domain-containing protein family member 1), which are suggested fusion tethering factors, and SNAREs, which carry the autophagosome-lysosome fusion out (Cheon

et al., 2019). The maturation of autophagosomes to autophagolysosomes is also dependent on RAB7 GTPase activity (Eskelinen, 2019).

Targets for autophagic degradation are tagged with p62 protein, also called SQSTM1 (sequestosome 1) (Hamano *et al.*, 2008), which serves as a cargo targeting protein. Targets of autophagy, such as misfolded and/or aggregated protein, can be tagged with p62 either by being tagged with multiple ubiquitin molecules first and by p62 through its ubiquitin-binding domain second (Hamano *et al.*, 2008) or without the need for ubiquitin chain (Watanabe and Tanaka, 2011). p62-tagged cargo is then recognized by LC3-II and engulfed by phagophore (Glick *et al.*, 2010) and is degraded in the process by autophagy (Yue *et al.*, 2009).

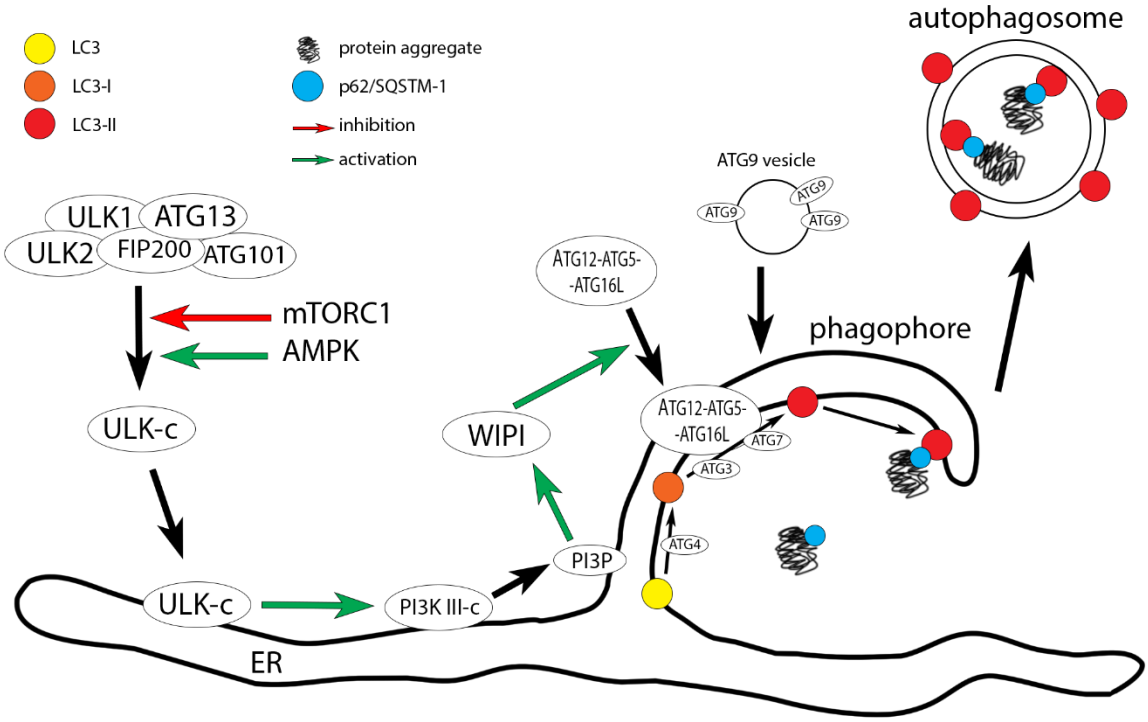

Figure 4: Mechanism of phagophore formation and creation of autophagosome with misfolded protein

3.3.3 Autophagy regulation

Autophagy is stimulated upon cells being afflicted with stress conditions. Amino-acid starvation is best understood (Eskelinen, 2019), other conditions affecting autophagy include hypoxia, oxidative stress, ER stress, or lack of growth factors (Cheon *et al.*, 2019; Eskelinen, 2019; Parzych and Klionsky, 2013). One of the pathways of autophagy regulation is dependent on the number of carbon nutrients and is executed by the cAMP-dependent protein kinase A (PKA) pathway, and amino-acids carried out in TOR (target of rapamycin) pathway (Parzych and Klionsky, 2013). PKA pathway is an inhibitor of autophagy in yeast (Parzych and Klionsky, 2013). Mammalian target of rapamycin (mTORC1) also inhibits autophagy and is positively affected by amino-acids (Parzych and Klionsky, 2013). A deficit in amino-

acids leads to inactivation of mTORC1 and ULK1 becomes dephosphorylated and goes through autophosphorylation (Eskelinen, 2019). ULK1 then phosphorylates other ULK complex proteins, which spurs ULK complex translocation to phagophore (Eskelinen, 2019). Autophagy is also regulated by the energy reserve levels by ATP/AMP ratio. This is performed by AMP-activated protein kinase (AMPK) sensing the levels of AMP, which activates AMPK kinase activity (Glick *et al.*, 2010; Parzych and Klionsky, 2013), and so AMPK can influence autophagy. Either via promoting the inhibitory activity of Tsc1/Tsc2 proteins on a GTPase Rheb required for mTORC1 function and inhibiting mTORC1 indirectly (Glick *et al.*, 2010; Parzych and Klionsky, 2013) or by inducing phosphorylation of ULK1 and other proteins to induce autophagy (Eskelinen, 2019; Parzych and Klionsky, 2013). AMPK can also inhibit mTORC1 directly (Parzych and Klionsky, 2013).

3.3.4 Autophagy in Alzheimer's disease

Earlier studies found the accumulation of autophagosomes in the brains of patients with neurodegenerative disease, which led to the conclusion that autophagy contributed to pathology (Levine and Kroemer, 2008). On the contrary, autophagy in neurons is high under physiological conditions, though it may deteriorate with age (Eskelinen, 2019), which may facilitate neurodegeneration (Hipp *et al.*, 2019). In mice neural-cell-specific autophagy-proteins-knockout models, mice developed severe neurodegeneration, progressive motor decline, behavioral changes, and shortened lifespan (Eskelinen, 2019). Neurodegenerative diseases like AD are characterized by the presence of aggregated tau and amyloid-β and studies indicate the crucial role of autophagy in their clearance (Eskelinen, 2019; Levine and Kroemer, 2008). Aggregated proteins are not a suitable target for proteasomal degradation since protein must be unfolded to fit into proteasome pore (Levine and Kroemer, 2008), and with age, misfolded protein levels increase due to oxidative stress and chaperone depletion, especially in post-mitotic, nondividing cells like neurons (Hipp *et al.*, 2019). This can be aggravated by mutations in aggregation-prone proteins (Hipp *et al.*, 2019). A study conducted on the post-mortem brains of AD patients indicated autophagy dysfunction (Caberlotto *et al.*, 2019). High cholesterol, which is present in neurodegenerative patient's brains - AD brains included, has shown to inhibit autophagy through autophagosome-lysosome function, even though it stimulates autophagosome formation (Eskelinen, 2019). APP and PSN1 mutant neurons exhibit impaired autophagy and lysosomal function. When β-secretase, an enzyme important for APP cleavage and formation of harmful forms of amyloid-β, was inhibited, the lysosomal function was restored. Another study conducted on mice showed that hippocampal neurons expressing AD-related mutant APP have damaged autophagy and mitophagy (Eskelinen, 2019), which could further worsen aggregation by oxidative stress caused by flawed mitochondria. Studies conducted on *Caenorhabditis elegans*, *Drosophila*, and mice found that knockdown of Rubicon - a negative regulator of autophagy - increases the lifespan and even helps in decreasing aging-associated phenotypes, furthermore restoring autophagy in old mice brains was able to reverse age-related memory loss (Eskelinen, 2019).

3.3.5 Tau aggregation and Autophagy

Tau is degraded by both proteasomal pathway and autophagy. Studies have shown that proteasome has only a minor role in tau degradation. Only inactivation of autophagy led to tau aggregate accumulation, and proteasome inhibition led to degradation of tau by autophagy, as detected by an increase in LC3-II and a large presence ofautophagosomes (Krüger *et al.*, 2012; Wang *et al.*, 2010). Also, hyperphosphorylated tau has been found colocalized with both LC3 and p62/SQSTM1 in patient brains afflicted with PSP, CBD, and familial AD (Piras *et al.*, 2016). However, some authors suggest that proteasome may be important for the degradation of soluble, monomeric, unphosphorylated tau (Samimi *et al.*, 2020). Tau pathology seems to be upstream event leading to defective autophagy since the autophagy needs proper trafficking alongside microtubules (either for autophagosome maturation or its fusion with lysosomes), which, in case of dysfunctional tau in tauopathies, may be incapacitated (Liu and Li, 2019; Samimi *et al.*, 2020).

Tau can be degraded by autophagy regardless of its posttranslational modifications (Wang and Mandelkow, 2012) by either macroautophagy or chaperone-mediated autophagy (CMA). Nonetheless, whether tau is destined for macroautophagy or CMA may be dependent on its inner structure. The study of Caballero *et al*. (2018) has presented differences between isoforms, as well as in different mutations. In different isoforms, the number of N-terminal domains is important (Fig. 5). 0N tau isoforms had decreased uptake by lysosomes but the uptake of 1N isoforms was faster. The number of microtubule-binding repeats had no effect. Considering mutations, A152T was preferably degraded by CMA, however, this mutation was able to reroute to macroautophagy. P301L mutation displayed no ability to reroute and be degraded by macroautophagy. Surprisingly, these mutant tau species have shown to enhance overall protein turnover, possibly as a coping mechanism for aberrant proteins. Yet, their ability for autophagy exhibited a saturation cap, and when presented with other stressors, exhausted proteolytic systems could not cope with them properly. This may further aggravate tauopathies by making neurons more susceptible to chronic cellular stress. However, macroautophagy and CMA may be antagonistic in coping with tauopathies (Wang and Mandelkow, 2012). Macroautophagy serves as a route to degrade tau aggregates. On the other hand, CMA may lead to toxic tau cleavage, and thus producing aggregation-prone fragments, exacerbating the pathology (Wang *et al.*, 2010; Wang and Mandelkow, 2012). Furthermore, it is possible that in tauopathies, lysosomal integrity may be impaired (Piras *et al.*, 2016), debilitating autophagy even further.

Autophagic clearance of tau can be enhanced by stimulating autophagy, for example, by using rapamycin (thus inhibiting mTORC1 inhibitory activity on autophagy) or trehalose. (Piras *et al.*, 2016). However, the effect of autophagy activation depends on the type of cell culture. In cultured primary neurons, rapamycin has failed to activate autophagy, unlike trehalose. But surprisingly, in N2a cells, both rapamycin and trehalose activated autophagy, and trehalose treatment displayed a reduction

of endogenous tau and a great increase of autophagosomes (Krüger *et al.*, 2012). Considering different outcomes in different neuronal cell lines, and a diverse possibility of autophagic clearance of different tau species, it is possible that a specific autophagy stimulator is needed for distinct conditions. So far, rapamycin has been a promising target, lowering amyloid-β levels reducing amyloid plaques and NFTs, and preventing cognitive decline. However, after long-term inhibition of mTOR, rapamycin has toxic side-effects, making it not suitable for long-term use by patients (Liu and Li, 2019).

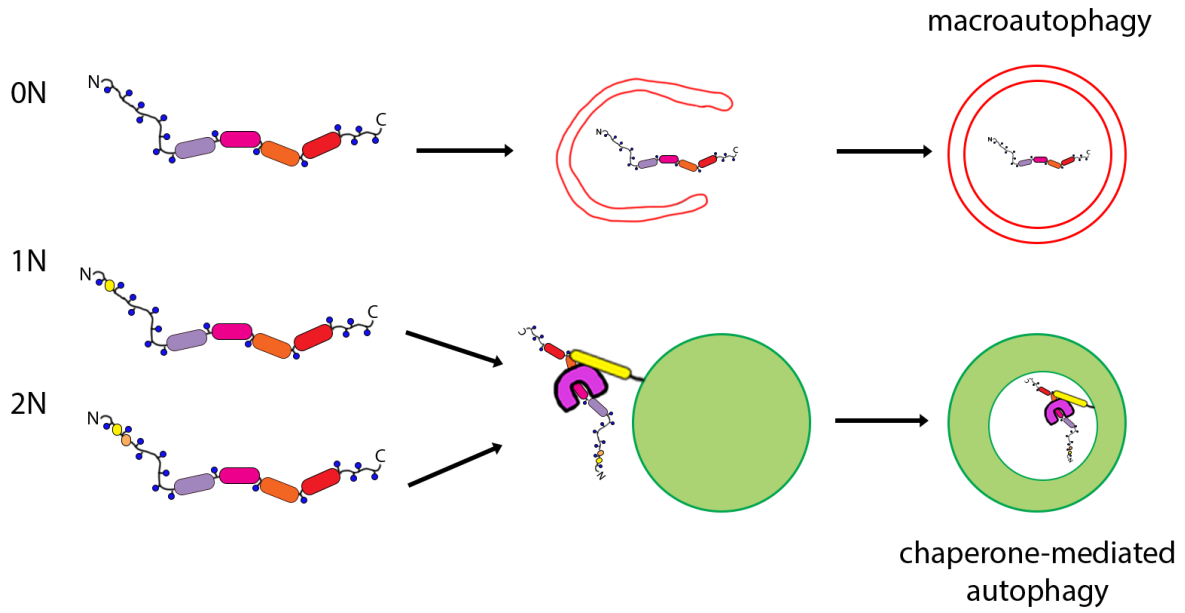

Figure 5: Degradation of hyperphosphorylated tau based on the number of N-terminal repeats (on the left), 0N tau is preferentially degraded by macroautophagy, whereas 1N and 2N are degraded by chaperone-mediated autophagy (chaperone - purple horseshoe), recognized by LAMP2A (yellow) and uptaken by lysosome (green) (according to Caballero *et al.*, 2018).

4 MATERIALS AND METHODS

4.1 Cell-line

- Tau RD P301S FRET Biosensor cells (ATCC® CRL-3275™)

4.2 Equipments

- Centrifuge 5810R (Eppendorf, Germany)
- ChemiDoc MP analyser (BioRad, USA)
- EnSpire Multimode Plate Reader (PerkinElmer Inc., USA)
- Electrophoresis and Blotting Vertical Apparatus (BioRad, USA)
- MSC-Advantage Biological Safety Cabinet (flow-box) (Thermo Fisher Scientific, USA)
- ViCell XR Cell Viability Analyzer (Beckman Coulter Inc., USA)
- iBlot 2 Dry Blotting System (Thermo Fisher Scientific, USA)
- Rotina 420 R Centrifuge (Hettich Zentrifugen) (Hettich, Germany)
- Prism 8 (GraphPad, USA)
- CO2 incubator

4.3 Chemicals and solutions

Chemicals

- 10x Tris/Glycine/SDS (Bio-Rad, #1610772]
- 30% Acrylamide/Bis-acrylamide 29:1 (Bio-Rad, #1610156)
- Resolving gel buffer 1.5 M Tris-HCl pH 8.8 (Bio-Rad, #161-0798)
- Stacking gel buffer 0.5 M Tris-HCl pH 6.8 (Bio-Rad, #161-0799)
- Tetramethylethylenediamine (TEMED) (Bio-Rad, #1610801)
- TrypLE™ Express Enzyme (1X), no phenol red (Thermo Fisher Scientific, #12604013)
- Bovine serum albumin (BSA) (Sigma-Aldrich, #A2153)
- Dulbecco's Modified Eagle Medium (Lonza, #12-604F)
- Epigallocatechin-3-gallate (EGCG), (Sigma-Aldrich, #E4143)
- GlutaMAX™ Supplement (Gibco, #35050061)
- jetPRIME® polyplus transfection kit (Polyplus infection, #114-15)
- Thiazolyl Blue Tetrazolium Bromide (MTT) (Sigma-Aldrich, # M2128)
- Pierce™ BCA Protein Assay Reagent A (Thermo Fisher Scientific, #23223)
- Pierce™ BCA Protein Assay Reagent B (Thermo Fisher Scientific, #23224)
- Protease Inhibitor Cocktail Tablets (Roche, #04693116001)
- PhosSTOP™ (Roche, #04906845001)
- Spectra™ Multicolor Broad Range Protein Ladder (Thermo Fisher Scientific, #26634)

Stocks

- 10x PBS: 80 g NaCl, 2.0 g KCl, 14.4 g Na_2HPO_4, 2.4 g KH_2PO_4 dissolved in 800 ml dH_2O, pH adjusted to 7.4 with HCl and added dH_2O to 1000 ml, sterilized by autoclaving.
- 10x TBS buffer: 24 g Tris base and 88 g NaCl dissolved in 900 ml dH_2O, pH adjusted to 7.6 with HCl and added dH_2O to 1 000 ml.
- TBST buffer: 1x TBS buffer with 0.1% Tween 20.
- RIPA buffer (radioimmunoprecipitation assay buffer): 150 mM sodium chloride, 1.0% NP-40, 0.5% sodium deoxycholate, 0.1% SDS (sodium dodecyl sulfate), 50 mM Tris, pH 8.0.
- 5× SDS loading buffer: 250 mM Tris-HCl (pH=6.8), 10% SDS, 30% glycerol, 0.5 M DTT, 0.02% Bromophenol Blue, 10% Mercaptoethanol.
- 0.05% Triton X-100 solution (10 mL): 1X TBS with 5 µL Triton X-100.
- 10% (w/v) SDS.
- 5% (w/v) BSA blocking solution: 2 g BSA dissolved in 30 ml of TBST buffer, added TBST to 40 ml.
- 10% resolving polyacrylamide gel (10 mL): 3.8 ml dH_2O, 3.4 ml 30% acrylamide/bis-acrylamide, 2.6 ml resolving gel buffer, 100 µl 10% (w/v) SDS, 100 µl 10% (w/v) APS, 10 µl TEMED.
- 12% resolving polyacrylamide gel (10 mL): 3.2 ml dH_2O, 4 ml 30% acrylamide/bis-acrylamide, 2.6 ml resolving gel buffer, 100 µl 10% (w/v) SDS, 100 µl 10% (w/v) APS, 10 µl TEMED.
- Stacking polyacrylamide gel (5 mL): 2.975 ml dH_2O, 670 µl 30% acrylamide/bis-acrylamide, 1.25 ml stacking gel buffer, 50 µl 10% (w/v) SDS, 50 µl 10% (w/v) APS, 5 µl TEMED.
- MTT stock: 5 mg MTT in 1 mL sterile PBS and filtered. Stored at -20°C.

4.4 Antibodies

- Rabbit Phospho-Tau (Ser262) Polyclonal Antibody (Thermo Fisher Scientific, #OPA1-03142)
- Rabbit anti-LAMP1 antibody (Cell signaling Technology, #9091)
- Rabbit anti-LC3A/B antibody (Cell signaling Technology, #4108)
- Mouse anti-p62 antibody (Cell signaling Technology, #88588)
- Mouse anti-β-actin antibody (Sigma-Aldrich, #A2228)
- Donkey anti-Mouse IgG (H+L) Highly Cross-Adsorbed Secondary Antibody, Alexa Fluor 488 (Thermo Fisher Scientific, #A-21202)
- Goat anti-Rabbit IgG (H+L) Highly Cross-Adsorbed Secondary Antibody, Alexa Fluor 488 (Thermo Fisher Scientific, #A-11034)

4.5 Methods

Cell culture

Tau P301S biosensor cells were purchased from the American Type Culture Collection and cultivated in complete Dulbecco's Modified Eagle's growth medium supplemented with 10% fetal bovine serum, 1% antibiotics (streptomycin and penicillin) and 1% GlutaMax at 37 °C in a humidified 5% CO2 incubator. Cells were passaged every 2 days when confluent. Cells were washed with 1x PBS and treated with TrypLE to facilitate cell detachment. Complete growth medium was added to cells to inactivate TrypLE. The cell suspension was centrifuged at 300 x g for 5 minutes. The sedimented cell pellet was resuspended in 5 mL of complete medium and counted by use of Vi-CELL XR Cell Counter (Beckman Coulter).

Seeding Tau P301S biosensor cells with Tau R3 aggregates by transfection and EGCG treatment

Cells were plated in 6-well plates (0.5 x 10^6 cells/mL, 2 mL of medium /well) and cultured at 37 °C in a 5 % CO2 incubator overnight. The transfection mixture was prepared using jetPRIME® Polyplus transfection kit. Hundred µL of jetPRIME® buffer and 4 µL of jetPRIME® reagent mixed with 100 nM Tau R3 aggregates were mixed and added per well. First, jetPRIME® buffer and Tau R3 aggregates were mixed by vortexing 10 seconds and jetPRIME® reagent was added and vortexed again for 10 seconds. The mixture was incubated for 10 minutes at room temperature. The cells were replaced with pre-warmed fresh complete growth medium, and then treated with equal volumes of transfection mixture. After 4 hours of transfection, the transfection media was removed, and the cells were replaced with pre-warmed fresh complete medium. Samples were collected at 3, 6, 9, 12, 24, 36, and 48 hours after transfection. For EGCG treatment, after 4 hours of transfection with R3 aggregates, the cells were washed with 1x PBS and treated with 50 and 100 µM EGCG and incubated at 37 °C in the 5 % CO2 incubator and cells were collected after 48 hours of treatment.

Determining the IC_{50} value of EGCG

The cell viability of Tau P301S biosensor cells in the presence of EGCG was tested by an MTT test (Zbožínková, 2015). For this, cells were plated in 96-well plates at a density of 5 x 10^4 cells/mL and incubated overnight at 37 °C in a 5 % CO2 incubator. A solution of 1mM EGCG in complete media was used as a starting concentration at 1:2 serial dilution. After the EGCG treatment, the cells were incubated at 37 °C in the 5 % CO2 incubator for 72 hours. 10 µL of MTT was added to each well and incubated at 37 °C for 3 hours. After 3 hours of MTT treatment, 100 µL of SDS was added to dissolve formazan crystals and the plates were kept at 37 °C overnight. Absorbance at 570 nm was measured and IC_{50} value was calculated using GraphPad Prism software.

Cell culture sample collection

When collecting the samples, the medium was collected in a 15 mL conical centrifuge tube, and cells were washed with 1x PBS and collected in the same centrifuge tube after washing. For cell detachment, 200 µL of TrypLE was used. When detached, TrypLE was inactivated by the complete growth medium and the cell suspension was collected and centrifuged at 300 x g for 5 minutes to pellet cells. The sedimented cell pellet was resuspended in 1 mL of 1 x PBS, transferred into a 1.5 mL centrifuge tube, and centrifuged for 5 minutes at 4 000 RPM. The supernatant was discarded and the sedimented cell pellet was stored in a -80 °C freezer.

Sample processing and protein quantification

RIPA lysis buffer was mixed with protease and phosphatase inhibitors, and 100 µL of lysis buffer was added to cell pellets and mixed gently. Samples were sonicated using a water bath sonicator for 3 minutes at 50% Amplitude with 15-sec pulse ON and 15-sec pulse OFF. After sonication, tubes were centrifuged at 12 000 RPM at 4 °C for 20 minutes and the supernatant was transferred to a new chilled 1.5 mL centrifuge tube. The remaining cell pellet was discarded.

Protein concentration in samples was quantified using a BCA protein assay kit (ThermoFisher Scientific). A set of protein standards using bovine serum albumin (2 000, 1 500, 1000, 750, 500, 250, 125, 25 and 0 µg/mL) were used for calibration. BCA reagent A and BCA reagent B were mixed at 50:1 ratio. 10 µL of each standard and 2.5 µL of samples were pipetted into separate wells and 200 µL of BCA reagent A and B mixture was added to each well. The plate was incubated at 37 °C for 30 minutes, and the absorbance was measured using an EnSpire Multimode Plate Reader (PerkinElmer) at 562 nm. The calibration curve was prepared in Microsoft Excel and sample protein concentration was calculated.

SDS-PAGE Electrophoresis and Western blotting

The volume of a quantified sample containing 40 µg of protein was calculated and it was added into a new 1.5 mL centrifuge tube. 3 µL of SDS gel loading dye supplemented with 10% β-mercaptoethanol per protein sample (15 µL) was added to protein sample containing tubes. RIPA buffer was added to bring the sample volume to 15 µL. This mixture of sample, dye, and buffer was heated at 95 °C for 5 minutes in a dry thermal block. After heating and letting it cool down, samples were quicks spun for 10 seconds and loaded on to gels. Samples were separated by 10% and 12% denaturing SDS polyacrylamide gel electrophoresis. Gels were hand cast using the Bio-Rad Mini-PROTEAN Tetra Cell system using Tris-Glycine-SDS buffer. Electrophoresis was run at 200 V for 1-1.5 hours approximately until the dye hit the bottom of the gel.

Western blotting was done using the iBlot 2 Dry Blotting System (ThermoFisher Scientific) and iBlot™ PVDF Transfer Stack (ThermoFisher Scientific), which contains methanol pre-activated membrane. The protein blot transfer time was 10-15 minutes at 20-25 Volts.

Blotted membranes were blocked in 5% BSA (diluted in 1x TBST buffer) for 1 hour. Membranes were quickly washed in 1x TBST for 1-2 minutes after blocking. Buffer was discarded after washing and membranes were treated with primary antibodies such as anti-LC3A/B, anti-p62, and anti-LAMP1 and anti-β actin primary antibodies and incubated overnight in 4 °C. After incubation, membranes were washed with 1x TBST 4 times with each wash at 10 minutes interval. The washing buffer was discarded after each wash. Then, membranes were treated with respective secondary antibodies (anti-mouse, anti-rabbit) conjugated with Alexa 488 fluorescent dye and incubated for 2 hours at room temperature on a shaker. The shaker speed maintained throughout this process at 120 RPM. Then, membranes were washed with 1x TBST 4 times with each wash at 10 minutes interval. After the final wash, membranes were imaged in the Bio-Rad Gel Documentation system and images were processed using ImageJ software.

5 RESULTS

5.1 Determining the IC_{50} value of EGCG

The IC_{50} value of EGCG (72 hours) for Tau P301S biosensor cells was determined as 101.8 μM using MTT assay and calculated using GraphPad Prism 8 (Fig. 6).

5.2 Seeding Tau P301S biosensor cells with Tau R3 aggregates

Tau P301S biosensor cells were seeded with Tau R3 aggregates resulted in the intracellular Tau P301S aggregate inclusions after 48-72 hours. The presence of intracellular tau aggregate inclusions was observed using the Operetta High-content imaging system (Fig. 9A,B).

5.3 Analysis of autophagy levels after seeding with Tau R3 aggregates

The level of autophagy induction was measured by quantifying the conversion of LC3A/B I to LC3A/B II. There was no autophagy induction in Tau P301S biosensor cells upon seeded with Tau R3 aggregates (Fig. 7A,D). p62 level increased upon induction with Tau R3 aggregates (Fig. 7B,E), which shows that the failure of autophagy induction upon Tau R3 aggregate-induced proteotoxic stress resulted in the aggregation of endogenous intracellular tau. There was no visible changes in the levels of LAMP1 after the tau aggreagtes transfection into Tau P301S biosensor cells (Fig. 7C,F).

5.4 EGCG induced autophagy reduced the level of Tau R3 aggregate induced triton-insoluble intracellular pSer262 Tau P301S aggregate

Introduction of extracellular Tau R3 aggregates resulted in the accumulation of triton-insoluble tau-RD aggregates in Tau P301S biosensor cells and the aggregated triton-insoluble tau fractions showed an increased tau phosphorylation at Ser262 (Fig. 10A,B). EGCG treatment at 50 μM (½ IC_{50}) and 100 μM (IC_{50}) reduced the Tau R3 aggregate-induced intracellular Tau-RD-P301S aggregation in biosensor cells confirmed by Operetta High-content imaging system (Fig. 9A,B). EGCG treatment induced autophagy was confirmed by western blot analysis of the conversion of LC3A/B II upon EGCG treatment (Fig. 8A,D). There was no visible changes observed in the levels of p62 and LAMP1 by western blot upon EGCG treatment (Fig. 8B,C & E,F). EGCG treatment induced autophagy reduced the level of triton-insoluble pSer262 tau P301S aggregates (Fig. 10A,B).

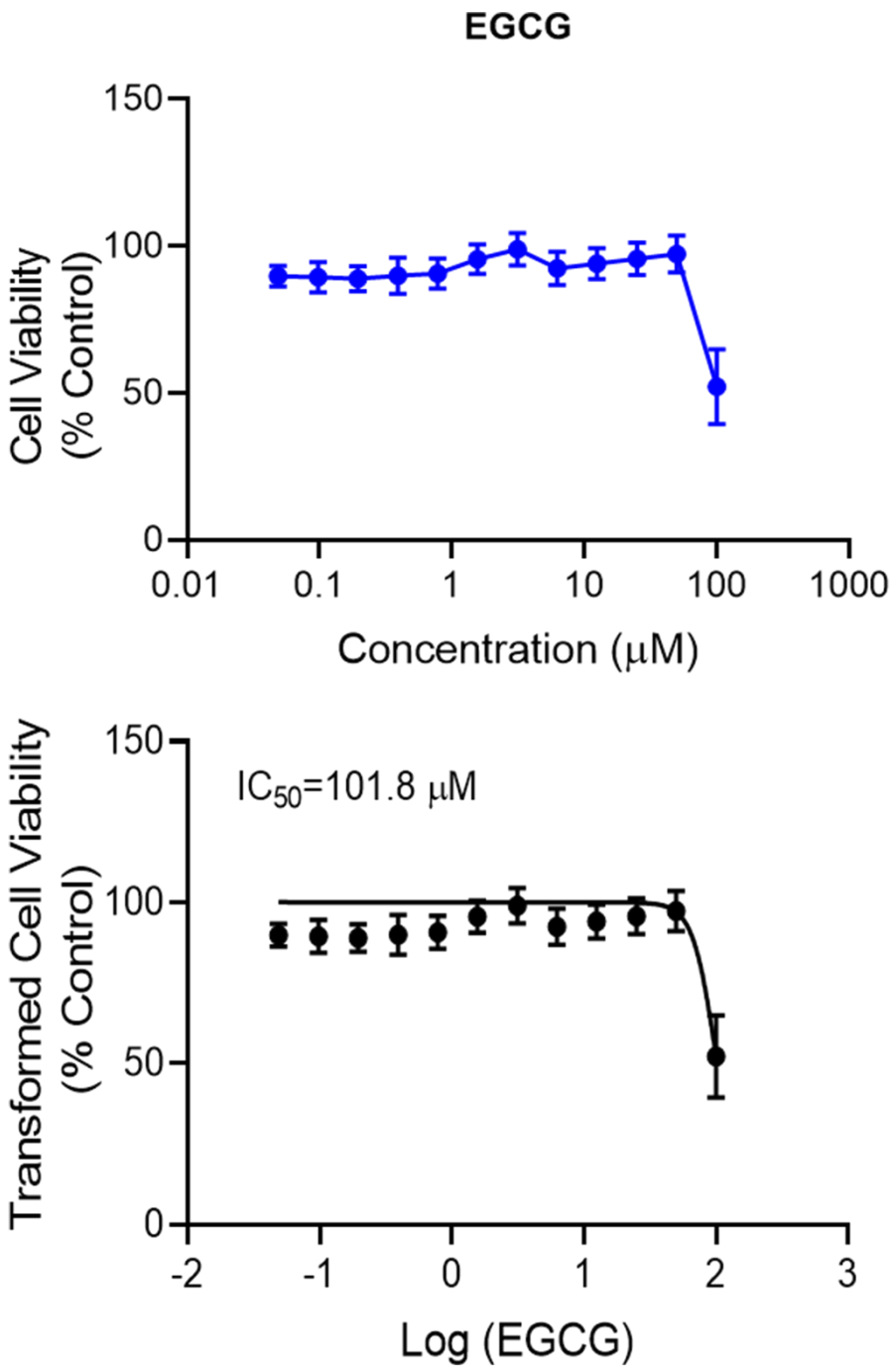

Figure 6: Effect of EGCG on cell viability. Data are shown as mean ± SEM, n = 3.

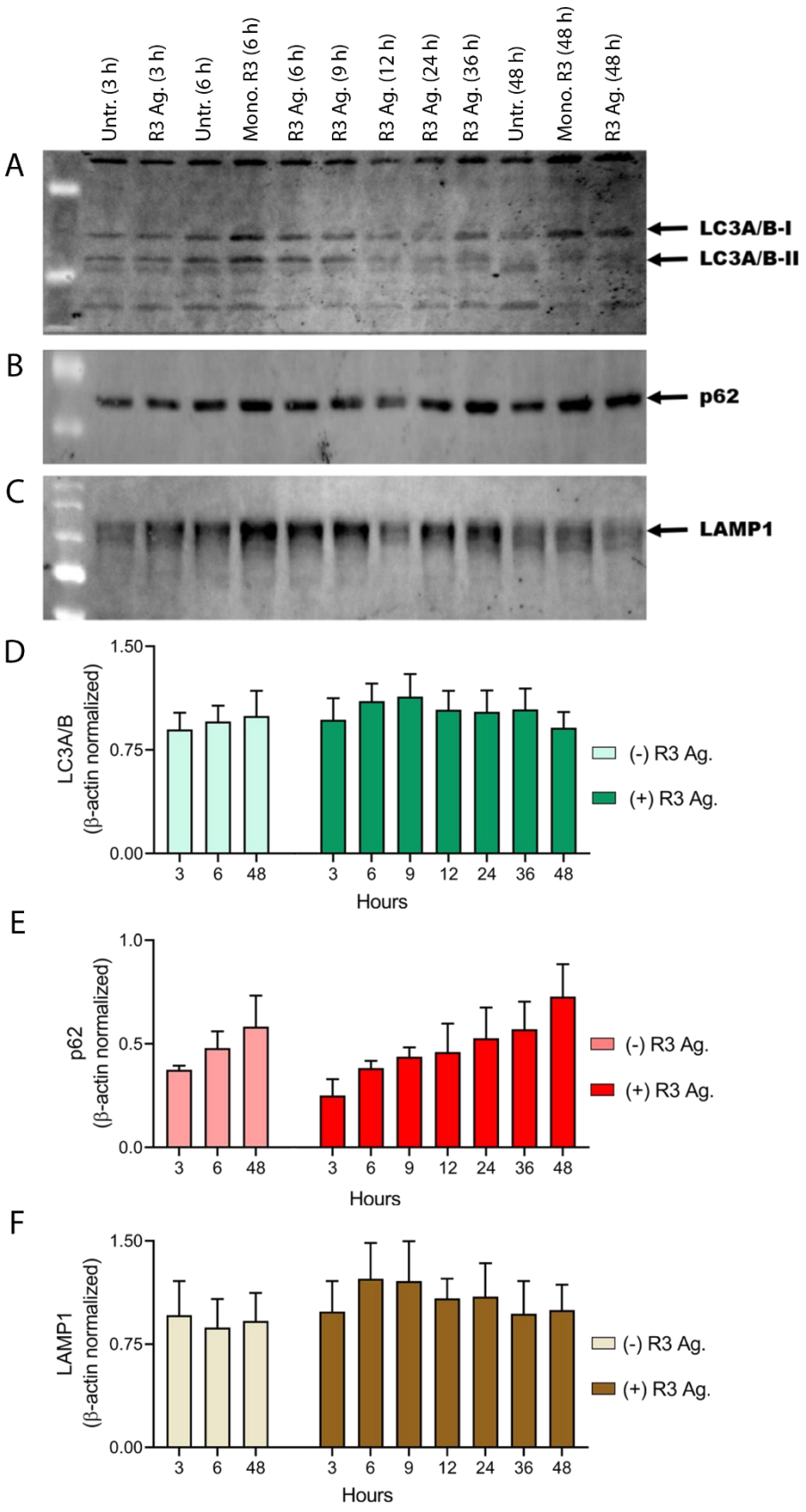

Figure 7: Western blot analysis of levels of LC3A/B (A, D), p62 (B, E), and LAMP1 (C, F) respectively, after tau R3 aggregates (R3 Ag.) transfection. Time (hours) in brackets shows time after the start of transfection. Untr./(-)R3 ag. - cells untreated/not seeded; Mono. R3- cells seeded with monomeric tau R3, (+)R3 Ag. - cells seeded with R3 aggregates. Data shown as mean ± SEM, n =2.

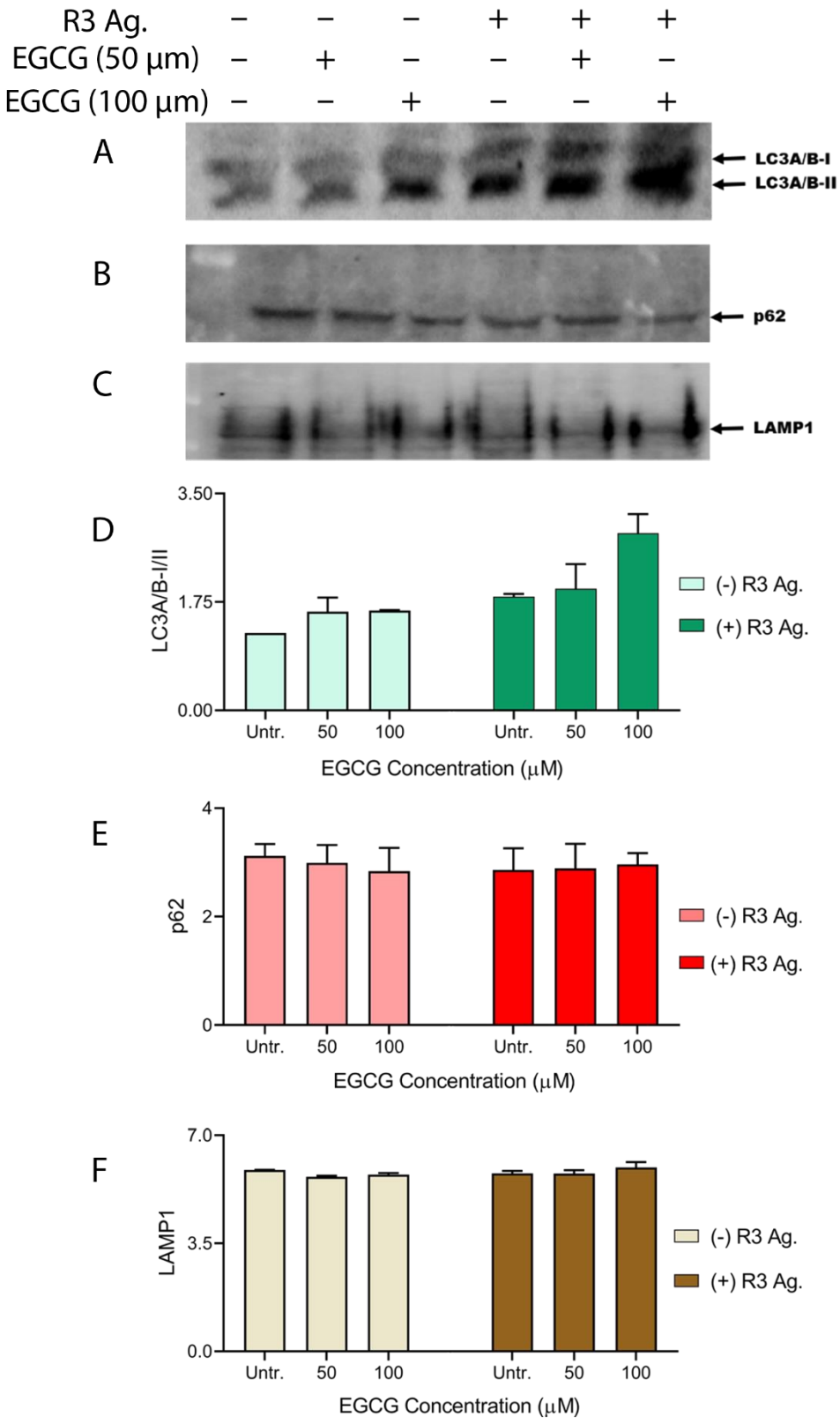

Figure 8: Western blot analysis of levels of LC3A/B (A, D), p62 (B, E), and LAMP1 (C, F), respectively, after 48 h EGCG treatment; (+) R3 Ag.- cells seeded with R3 aggregates, (-)R3 Ag.- cells not seeded with R3 aggregates; Untr.- cells not treated with EGCG. Data shown as mean ± SEM, n =2.

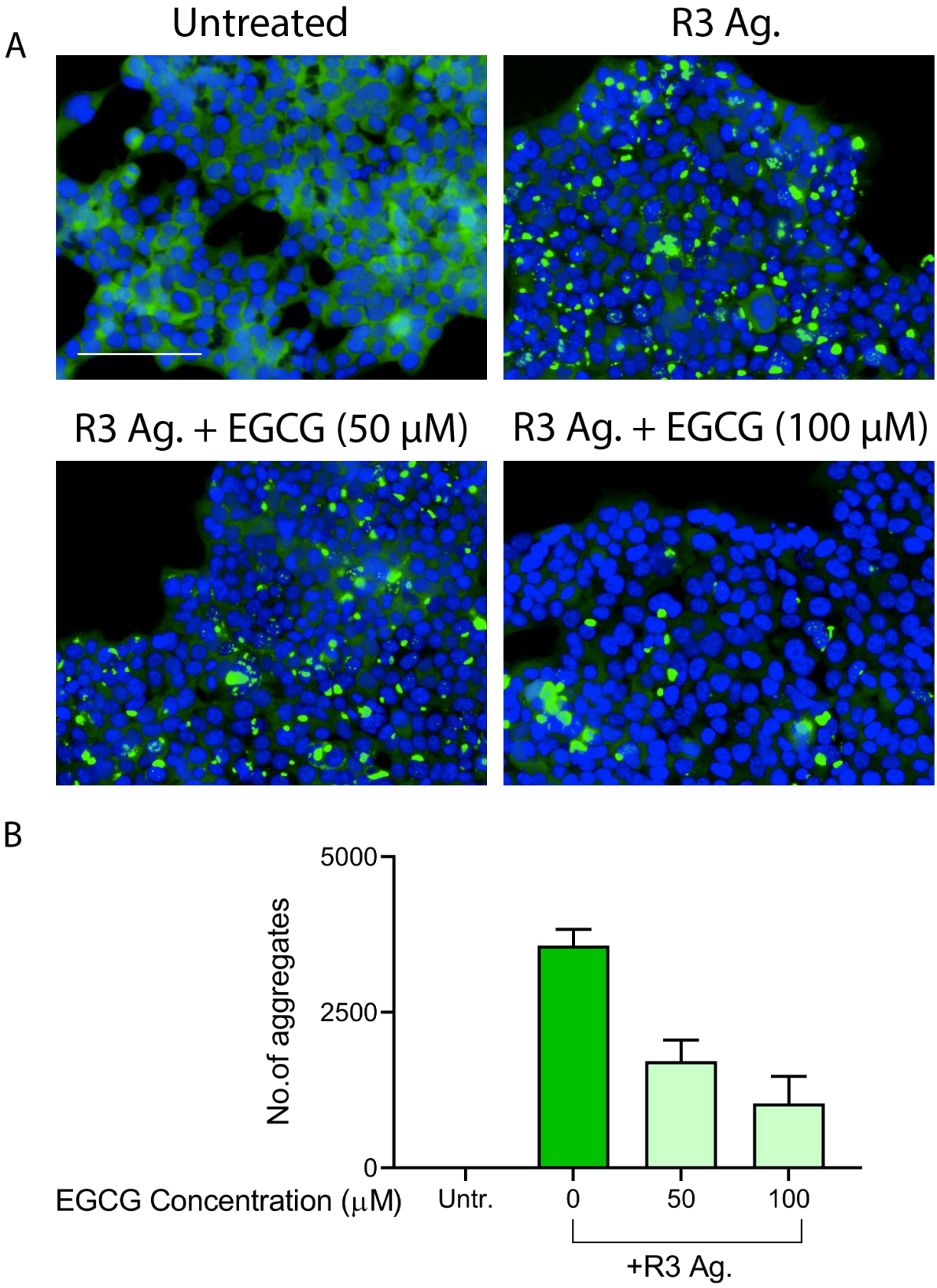

Figure 9: A- Intracellular R3 aggregates seeded tau aggregate inclusions (high intensity green spots) under EGCG treatment conditions. B- Analysis of number of tau aggregregates in R3 aggregates seeded tau P301S biosensor cells after EGCG treatment; Untr.- cells not treated with R3 Ag./EGCG. (+)R3 Ag.- cells seeded with R3 aggregates. Data shown as mean ± SEM, n =2. (Performed by Narendran Annadurai).

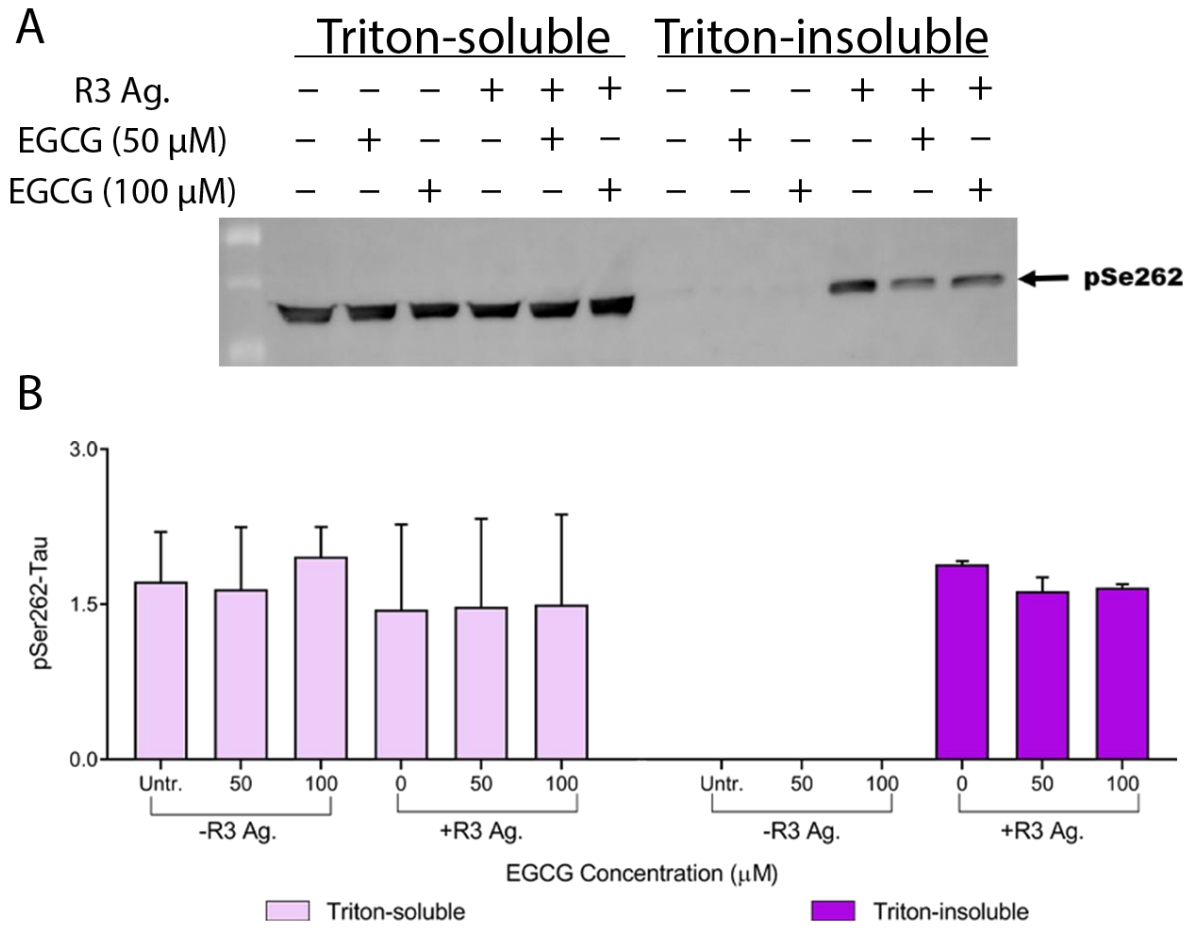

Figure 10: Western blot (A) and analysis of levels (B) of triton-soluble and triton-insoluble pSer262 tau; (+)R3 Ag.- cells seeded with R3 aggregates; (-)R3 Ag – cells not seeded with R3 aggregates, Untr.- cells not treated with R3Ag./EGCG. Data shown as mean ± SEM, n =2.

6 DISCUSSION

Intracellular tau aggregate formation and intracellular prion-like spreading of tau aggregate define the propagation and toxicity of tauopathies in neurodegenerative diseases. The formation of hyperphosphorylated intracellular tau aggregates resultin the proteotoxic stress in cells. Failure of cellular protein aggregate clearance mechanisms, such as autophagy and ubiquitination, increases the buildup of intracellular tau protein aggregates. Autophagy induction was also proposed to overcome the proteotoxic related cellular pathologies (Djajadikerta *et al.*, 2020). From our results, it is clear that EGCG induced autophagy in Tau RD P301S biosensor cells and increased autophagy reduced the level of intracellular pSer262 tau aggregates.We did not find a clear change in the levels of p62 and LAMP1 upon EGCG. Detailed studies are needed to clearly understand the mechanisms of how EGCG induces autophagy.

Several autophagy inducers are being tested in experimental and and clinical studies (Djajadikerta *et al.*, 2020), with good or better outcome. However, it is crucial to know the exact mechanism of autophagy induction and possible side-effects of long-term usage. For example, rapamycin, an mTOR inhibitor and promising tool in autophagy-induction treatment, is known to be toxic and not suitable for long-term use in chronically ill patients (Liu *et* Li, 2019). Therefore, we decided to test the effect of EGCG as it is already consumed by the general public since it is abundantly found in green tea leaves.

Chesser *et al.*(2016) conducted a study about EGCG and its effect on phosphorylated tau clearance. Their study was conducted on primary cortical rat neurons obtained from rat embryos and testing the soluble tau clearance. On the other hand, our study was conducted on a cultured cell-line and we observed a clearance of tau aggregates. Their study has shown that in primary cortical neurons, EGCG did not induce autophagy. This may be due to a very high level of basal autophagy in neurons, not like our cells transfected with R3 aggregates. However, they did confirm that EGCG significantly helped to clear phosphorylated tau, probably due to the induction of p62 expression. Given the differences, a comparative study with both soluble and insoluble tau forms, and both primary neurons and cultured cell-lines should be conducted to shed further light on this problem. In the end, our and their study come to a similar conclusion that EGCG may help in the treatment of tauopathies.

We hope that this study will help in future therapeutic approaches such as autophagy inducers in reducing tau aggregate formation and its propagation.

7 CONCLUSION

In this thesis, we show that in the presence of Tau R3 aggregates, cells are exposed to proteopathic stress, thus debilitating their clearance of pathological aggregates by autophagy. We have observed that EGCG-induced autophagy resulted in the clearance of endogenous pSer262 Tau P301S triton-insoluble aggregates, and their presence in the cells. These findings show us that EGCG, found in green tea, might be a possible future target for the treatment of tauopathies.

REFERENCES

Alberts, B., 2015. Molecular Biology of the Cell. New York: W.W. Norton & Company.

Andreadis, A., 2006. Misregulation of Tau Alternative Splicing in Neurodegeneration and Dementia. https://doi.org/10.1007/978-3-540-34449-0_5

Annadurai, N., Cagnotto, A., Bastone, A., Salmona, M., Džubák, P., Hajdúch, M., Das, V., 2017. Identification of potential inhibitors of tau aggregation for Alzheimer's disease therapy. Chemické Listy, Czech Chemical Society Symposium Series Vol. 15, 1, 1–48.

Barbier, P., Zejneli, O., Martinho, M., Lasorsa, A., Belle, V., Smet-Nocca, C., Tsvetkov, P.O., Devred, F., Landrieu, I., 2019. Role of Tau as a Microtubule-Associated Protein: Structural and Functional Aspects. Frontiers in Aging Neuroscience 11, 204. https://doi.org/10.3389/fnagi.2019.00204

Caballero, B., Wang, Y., Diaz, A., Tasset, I., Juste, Y.R., Stiller, B., Mandelkow, E.-M., Mandelkow, E., Cuervo, A.M., 2018. Interplay of pathogenic forms of human tau with different autophagic pathways. Aging Cell 17, e12692. https://doi.org/10.1111/acel.12692

Caberlotto, L., Nguyen, T.-P., Lauria, M., Priami, C., Rimondini, R., Maioli, S., Cedazo-Minguez, A., Sita, G., Morroni, F., Corsi, M., Carboni, L., 2019. Cross-disease analysis of Alzheimer's disease and type-2 Diabetes highlights the role of autophagy in the pathophysiology of two highly comorbid diseases. Scientific Reports 9, 3965. https://doi.org/10.1038/s41598-019-39828-5

Cheon, S.Y., Kim, H., Rubinsztein, D.C., Lee, J.E., 2019. Autophagy, Cellular Aging and Age-related Human Diseases. Exp Neurobiol 28, 643–657. https://doi.org/10.5607/en.2019.28.6.643

Cohen, T.J., Constance, B.H., Hwang, A.W., James, M., Yuan, C.-X., 2016. Intrinsic Tau Acetylation Is Coupled to Auto-Proteolytic Tau Fragmentation. PLOS ONE 11, e0158470. https://doi.org/10.1371/journal.pone.0158470

Cohen, T.J., Friedmann, D., Hwang, A.W., Marmorstein, R., Lee, V.M.Y., 2013. The microtubule-associated tau protein has intrinsic acetyltransferase activity. Nature Structural & Molecular Biology 20, 756–762. https://doi.org/10.1038/nsmb.2555

Dickson, D.W., Kouri, N., Murray, M.E., Josephs, K.A., 2011. Neuropathology of Frontotemporal Lobar Degeneration-Tau (FTLD-Tau). Journal of Molecular Neuroscience 45, 384–389. https://doi.org/10.1007/s12031-011-9589-0

Elie, A., Prezel, E., Guérin, C., Denarier, E., Ramirez-Rios, S., Serre, L., Andrieux, A., Fourest-Lieuvin, A., Blanchoin, L., Arnal, I., 2015. Tau co-organizes dynamic microtubule and actin networks. Scientific Reports 5, 9964. https://doi.org/10.1038/srep09964

Eskelinen, E.-L., 2019. Autophagy: Supporting cellular and organismal homeostasis by self-eating. The International Journal of Biochemistry & Cell Biology 111, 1–10. https://doi.org/10.1016/j.biocel.2019.03.010

Fan, L., Mao, C., Hu, X., Zhang, S., Yang, Z., Hu, Z., Sun, H., Fan, Y., Dong, Y., Yang, J., Shi, C., Xu, Y., 2020. New Insights Into the Pathogenesis of Alzheimer's Disease. Frontiers in Neurology 10, 1312. https://doi.org/10.3389/fneur.2019.01312

Georgieva, E.R., Xiao, S., Borbat, P.P., Freed, J.H., Eliezer, D., 2014. Tau Binds to Lipid Membrane Surfaces via Short Amphipathic Helices Located in Its Microtubule-Binding Repeats. Biophysical Journal 107, 1441–1452. https://doi.org/10.1016/j.bpj.2014.07.046

Gibbons, G.S., Lee, V.M.Y., Trojanowski, J.Q., 2019. Mechanisms of Cell-to-Cell Transmission of Pathological Tau: A Review. JAMA Neurology 76, 101–108. https://doi.org/10.1001/jamaneurol.2018.2505

Glick, D., Barth, S., Macleod, K.F., 2010. Autophagy: cellular and molecular mechanisms. The Journal of Pathology 221, 3–12. https://doi.org/10.1002/path.2697

Guo, T., Noble, W., Hanger, D.P., 2017. Roles of tau protein in health and disease. Acta Neuropathologica 133, 665–704. https://doi.org/10.1007/s00401-017-1707-9

Hamano, T., Gendron, T.F., Causevic, E., Yen, S.-H., Lin, W.-L., Isidoro, C., DeTure, M., Ko, L., 2008. Autophagic-lysosomal perturbation enhances tau aggregation in transfectants with induced wild-type tau expression. European Journal of Neuroscience 27, 1119–1130. https://doi.org/10.1111/j.1460-9568.2008.06084.x

Hanger, D.P., Anderton, B.H., Noble, W., 2009. Tau phosphorylation: the therapeutic challenge for neurodegenerative disease. Trends in Molecular Medicine 15, 112–119. https://doi.org/10.1016/j.molmed.2009.01.003

Hanger, D.P., Byers, H.L., Wray, S., Leung, K.-Y., Saxton, M.J., Seereeram, A., Reynolds, C.H., Ward, M.A., Anderton, B.H., 2007. Novel Phosphorylation Sites in Tau from Alzheimer Brain Support a Role for Casein Kinase 1 in Disease Pathogenesis. Journal of Biological Chemistry 282, 23645–23654. https://doi.org/10.1074/jbc.M703269200

Hipp, M.S., Kasturi, P., Hartl, F.U., 2019. The proteostasis network and its decline in ageing. Nature Reviews Molecular Cell Biology 20, 421–435. https://doi.org/10.1038/s41580-019-0101-y

Ishizawa, T., Mattila, P., Davies, P., Wang, D., Dickson, D.W., 2003. Colocalization of Tau and Alpha-Synuclein Epitopes in Lewy Bodies. Journal of Neuropathology & Experimental Neurology 62, 389–397. https://doi.org/10.1093/jnen/62.4.389

Jucker, M., Walker, L.C., 2013. Self-propagation of pathogenic protein aggregates in neurodegenerative diseases. Nature 501, 45.

Karran, E., Mercken, M., Strooper, B.D., 2011. The amyloid cascade hypothesis for Alzheimer's disease: an appraisal for the development of therapeutics. Nature Reviews Drug Discovery 10, 698–712. https://doi.org/10.1038/nrd3505

Krüger, U., Wang, Y., Kumar, S., Mandelkow, E.-M., 2012. Autophagic degradation of tau in primary neurons and its enhancement by trehalose. Neurobiology of Aging 33, 2291–2305. https://doi.org/10.1016/j.neurobiolaging.2011.11.009

Lawrence I. Golbe, 2014. Progressive Supranuclear Palsy. Semin Neurol 34(02), 151–159. https://doi.org/DOI: 10.1055/s-0034-1381736

Levine, B., Kroemer, G., 2008. Autophagy in the Pathogenesis of Disease. Cell 132, 27–42. https://doi.org/10.1016/j.cell.2007.12.018

Li, W., Lee, V.M.-Y., 2006. Characterization of Two VQIXXK Motifs for Tau Fibrillization in Vitro. Biochemistry 45, 15692–15701. https://doi.org/10.1021/bi061422+

Liu, J., Li, L., 2019. Targeting Autophagy for the Treatment of Alzheimer's Disease: Challenges and Opportunities. Frontiers in Molecular Neuroscience 12, 203. https://doi.org/10.3389/fnmol.2019.00203

Parzych, K.R., Klionsky, D.J., 2013. An Overview of Autophagy: Morphology, Mechanism, and Regulation. Antioxidants & Redox Signaling 20, 460–473. https://doi.org/10.1089/ars.2013.5371

Pierzynowska, K., Gaffke, L., Cyske, Z., Puchalski, M., Rintz, E., Bartkowski, M., Osiadły, M., Pierzynowski, M., Mantej, J., Piotrowska, E., Węgrzyn, G., 2018. Autophagy stimulation as a promising approach in treatment of neurodegenerative diseases. Metabolic Brain Disease 33, 989–1008. https://doi.org/10.1007/s11011-018-0214-6

Piras, A., Collin, L., Grüninger, F., Graff, C., Rönnbäck, A., 2016. Autophagic and lysosomal defects in human tauopathies: analysis of post-mortem brain from patients with familial Alzheimer disease, corticobasal degeneration and progressive supranuclear palsy. Acta Neuropathologica Communications 4, 22. https://doi.org/10.1186/s40478-016-0292-9

Rodríguez-Martín, T., Cuchillo-Ibáñez, I., Noble, W., Nyenya, F., Anderton, B.H., Hanger, D.P., 2013. Tau phosphorylation affects its axonal transport and degradation. Neurobiology of Aging 34, 2146–2157. https://doi.org/10.1016/j.neurobiolaging.2013.03.015

Rubinsztein, D.C., 2006. The roles of intracellular protein-degradation pathways in neurodegeneration. Nature 443, 780–786. https://doi.org/10.1038/nature05291

Samimi, N., Asada, A., Ando, K., 2020. Tau Abnormalities and Autophagic Defects in Neurodegenerative Disorders; A Feed-forward Cycle. Galen Medical Journal 9, 1681. https://doi.org/10.31661/gmj.v9i0.1681

Scheltens, P., Blennow, K., Breteler, M.M.B., de Strooper, B., Frisoni, G.B., Salloway, S., Van der Flier, W.M., 2016. Alzheimer's disease. The Lancet 388, 505–517. https://doi.org/10.1016/S0140-6736(15)01124-1

Seidler, P.M., Boyer, D.R., Rodriguez, J.A., Sawaya, M.R., Cascio, D., Murray, K., Gonen, T., Eisenberg, D.S., 2018. Structure-based inhibitors of tau aggregation. Nature Chemistry 10, 170–176. https://doi.org/10.1038/nchem.2889

Selkoe, D.J., Hardy, J., 2016. The amyloid hypothesis of Alzheimer's disease at 25 years. EMBO Molecular Medicine 8, 595–608. https://doi.org/10.15252/emmm.201606210

Wang, Y., Krüger, U., Mandelkow, E., Mandelkow, E.-M., 2010. Generation of Tau Aggregates and Clearance by Autophagy in an Inducible Cell Model of Tauopathy. Neurodegenerative Diseases 7, 103–107. https://doi.org/10.1159/000285516

Wang, Y., Mandelkow, E., 2016. Tau in physiology and pathology. Nature Reviews Neuroscience 17, 22–35. https://doi.org/10.1038/nrn.2015.1

Wang, Y., Mandelkow, E., 2012. Degradation of tau protein by autophagy and proteasomal pathways. Biochemical Society Transactions 40, 644–652. https://doi.org/10.1042/BST20120071

Watanabe, Y., Tanaka, M., 2011. p62/SQSTM1 in autophagic clearance of a non-ubiquitylated substrate. J. Cell Sci. 124, 2692. https://doi.org/10.1242/jcs.081232

World Alzheimer Report 2019: Attitudes to dementia., 2019. Alzheimer's Disease International, London, UK.

Yue, Z., Friedman, L., Komatsu, M., Tanaka, K., 2009. The cellular pathways of neuronal autophagy and their implication in neurodegenerative diseases. Biochimica et Biophysica Acta (BBA) - Molecular Cell Research 1793, 1496–1507. https://doi.org/10.1016/j.bbamcr.2009.01.016

Zhang, X., Gao, F., Wang, D., Li, C., Fu, Y., He, W., Zhang, J., 2018. Tau Pathology in Parkinson's Disease. Frontiers in Neurology 9, 809. https://doi.org/10.3389/fneur.2018.00809